Spring 2010

Evaluation of selected warm mix asphalt additives

Nishant Mukeshkumar Sheth
University of Iowa

EVALUATION OF SELECTED WARM MIX ASPHALT ADDITIVES

by

Nishant Mukeshkumar Sheth

A thesis submitted in partial fulfillment
of the requirements for the Master of
Science degree in Civil and Environmental Engineering
in the Graduate College of
The University of Iowa

May 2010

Thesis Supervisor: Associate Professor Hosin Lee

Graduate College
The University of Iowa
Iowa City, Iowa

CERTIFICATE OF APPROVAL

_____

MASTER'S THESIS

_____

This is to certify that the Master's thesis of

Nishant Mukeshkumar Sheth

has been approved by the Examining Committee
for the thesis requirement for the Master of Science
degree in Civil and Environmental Engineering at the May 2010 graduation.

Thesis Committee: _____
Hosin Lee, Thesis Supervisor

_____
James W Stoner

_____
Paul F Hanley

Be passionate about what you desire and the whole universe will conspire for your achievement - Paulo Chohelo, The Alchemist

ACKNOWLEDGMENTS

I am heartily thankful to my academic advisor, Dr. Hosin Lee, whose encouragement, guidance and support from the initial to the final level enabled me to develop an understanding of the subject. I owe my deepest gratitude to Dr. Youngjoo Kim, who supervised me throughout my research. I would like to thank David Blanco for his help in doing experiments.

I would like to show my gratitude to Dharmsinh Desai University and University of Iowa for creating a lifetime opportunity for me to pursue BE-MS joint program. My special thanks to Dr. V.C. Patel, Dr. H.M. Desai and Dr. P. Barry Butler.

I am heartly thankful to the Public Policy Center, who provided financial support to me throughout my graduate study. My association with my academic advisor, Dr. Hosin Lee and Dr. Paul F Hanley has been greatly cherished. This thesis would not have been possible without Dr. Lee and Dr. Hanley's generous support. The core fundamentals learned from Dr. Wilfrid Nixon as well as Dr. James Stoner were extremely helpful throughout my graduate study.

Lastly, I offer my regards and blessings to all of those who supported me in any respect during the completion of the project.

.

ABSTRACT

Warm mix asphalt (WMA) is an emerging technology that can allow asphalt to be produced and compacted at a significantly lower temperature. In the past, a number of researchers evaluated various WMA mixtures using select testing procedures in the laboratory. However, none of them evaluated all four major WMA products and compared them against both control HMA and WMA mixtures without an additive using a comprehensive set of testing protocols. This thesis presents a comprehensive evaluation result of four major WMA additives regarding their tensile strength, moisture sensitivity, dynamic modulus and flow number.

The WMA specimens exhibited similar air voids as HMA specimens which indicate that WMA additives are effective in compacting asphalt mixtures at a lower temperature. The indirect tensile strengths and tensile strength ratio (TSR) values of all WMA specimens were lower than that of HMA specimens. This result indicates that WMA mixtures could be susceptible to moisture damage. The only WMA mixture with CECABSE RT® exhibited the higher dynamic modulus at 37.8°C than the control HMA mixture. All WMA specimens, except Advera WMA and CECABASE RT®, passed the requirement of 10,000 cycles of repeated loading. Particularly, the WMA mixture with granular Aspha-min® exhibited the lowest permanent deformation followed by the control HMA mixture.

The nano-scale images of additives with asphalt were also taken to study the characterization and interaction of WMA additives with asphalt. A shape resembling bee was observed in all asphalt images which has been criticized by the researchers. However, bee structures were disappeared in those images of asphalt with CECABASE

RT® additive. At nano-scale, height and phase angle of all additive were found greater than the asphalt which proves them highly viscous than the asphalt.

TABLE OF CONTENTS

LIST OF TABLES

LIST OF FIGURES

CHAPTER 1 INTRODUCTION AND LITERATURE REVIEW

Today, Transportation has proved to be a major contributor to the GDP and economy. It has grown, using the available nonrenewable natural resources, to the extent where the significant changes are required to make it sustainable. World crude oil demand grew an average of 1.76% per year from 1994 to 2006, with a high of 3.4% in 2003-2004 as per the U.S. Energy Information Administration [17]. World demand for oil is projected to increase 37% over 2006 levels by 2030, according to the 2007 U.S. Energy Information Administration's (EIA) annual report [17]. Transportation is one of the major global consumers of energy, currently representing between 20% to 25% of aggregate energy consumption and CO_2 emissions and a strong growth has been projected in all sectors with the same proportion from Transportation [40]. Tranport and especially road vehicles are major source of all pollutants like Nitrogen Oxides (Precursor to ozone pollution), VOC (Volatile Organic Compounds) and fine particulates [39]. 47 % of oxides of Nitrogen, 39 % of VOCs, and 66% of CO (Carbon Monoxide) emissions are produced by motor vehicle in Europe while the same in United States of America are 45%, 37% and 78% respectively [38].

We need to realize that we have been using environment as the waste assimilator and benefits from general environment resources and services. The transportation sector bears a major share of the responsibility of the problem which could be acid deposition, global warming, metropolitan ozone and urban air pollution or thinning stratospheric ozone level or holes in that layer to name a few [10].

94% of the United States paved road network is made up from the Hot Mix Asphalt [22]. The higher production and compaction temperature of the asphalt mix results emissions. The major source of emissions associated with the Hot Mix asphalt are the dryers, hot bins, and mixers, which emit particulate matter (PM) and a variety of gaseous pollutants. The storage silos, truck load-out operations liquid asphalt storage

tanks and yard emissions are also other sources associated with HMA. There are also minor emissions results from aggregate storage and handling operations, vehicle exhaust etc [23].

The PM emissions associated with HMA production include the criteria pollutants PM-10 (PM less than 10 micrometers in aerodynamic diameter) and PM-2.5, hazardous air pollutant (HAP) metals, and HAP organic compounds. The gaseous emissions associated with HMA production include the criteria pollutants sulfur dioxide (SO_2), nitrogen oxides (NO_x), carbon monoxide (CO), and volatile organic compounds (VOC), as well as volatile HAP organic compounds.

Absolute emerging technologies that appear to allow a reduction in the temperatures at which Asphalt mixes are produced and placed. These technologies have been labeled Warm Mix Asphalt (WMA). The immediate benefit to producing WMA is the reduction in energy consumption required by burning fuels to heat traditional hot mix asphalt (HMA) to temperatures in excess of 300° F at the production plant. These high production temperatures are needed to have good workability during laying and compaction, to make the asphalt binder viscous enough to completely coat the aggregate, and to achieve durability during traffic exposure. The decreased production temperature comes with the additional benefit of reduced emissions from burning fuels, fumes, and odors generated at the plant and the paving site. All these technologies appear to allow the production of WMA by reducing the viscosity of the asphalt binder at a given temperature. This reduced viscosity allows the aggregate to be fully coated at a lower temperature than what is traditionally required in HMA production. This technology could have a significant impact on transportation construction projects in and around non-attainment areas such as large metropolitan areas that have air quality restrictions. The

reduction in fuel usage to produce the mix would also have a significant impact on the cost of transportation construction projects. The benefits of these technologies to the United States in terms of energy savings and air quality improvements are promising but these technologies need further investigation and research in order to validate their expected performance and added value.

There are several benefits for using WMA such as the extension of the construction season and reduced aging of the asphalt binder. Reduction of the short term aging (oxidation and volatilization) of the asphalt binder during conventional construction could potentially enhance pavement performance through reduced thermal and fatigue cracking, thus decreasing the life cycle cost of the pavement. Its potential benefits include reduction in energy consumption, emissions, fumes, and odors while improving its performance. Due to its production and compaction at the lower temperatures, WMA pavements can be opened to traffic earlier than HMA pavements.

At the Bitumen Forum of Germany in 1997, WMA technology was identified as one of means to lower emissions. The WMA technology was introduced in the United States in 2002 when the NAPA sponsored an industry scanning tour to Europe for asphalt paving contractors [33]. In 2004, the World of Asphalt convention featured a demonstration project of WMA, and since then, WMA additive manufacturers have successfully performed many demonstration projects throughout the United States.

Three different WMA additives: Aspha-Min®, Sasobit® and Evotherm™ were evaluated and all three technologies were found to improve the compactibility of the asphalt mixture and resulted in lower air voids compared to HMA [19, 20, and 21]. It was reported that, based on Hamburg wheel-tracking test, these three WMA additives did

not increase the rutting potential [21]. It has been also reported that the accelerated WMA test sections exhibited the excellent field performance in terms of rutting [35].

Sasobit® [12] significantly reduced a permanent deformation based on the repeated creep recovery test. AC 60/70 binder modified with 3.0% Sasobit® not only improved the compactability but also exhibited a greater resistance to densification under simulated traffic [28]. Three types of CIR-foam specimens were prepared: (1) CIR-foam with 1.5% of Sasobit®, (2) CIR-foam with 0.3% Aspha-min®, and (3) CIR-foam without any additive [29]. They reported that WMA additives have improved the compactibility of CIR-foam mixtures resulting in a lower air void. The indirect tensile strength of CIR-foam mixtures with Sasobit® was the highest and the dynamic moduli of CIR-foam mixture with WMA additives were higher than ones without any additive. Flow number of CIR-foam mixtures with Sasobit® was the highest followed by ones with Aspha-min® and ones without any additive.

CHAPTER 2 LABORATORY EXPERIMENTS WITH DIFFERENT WARM MIX ASPHALT ADDITIVES

Objective

To provide a safe and reliable highway, warm mix asphalt (WMA) pavement must meet requirements for strength, moisture sensitivity, stiffness and rutting. The main objective of this research is to 1) investigate the available technologies for producing WMA and 2) evaluate selected WMA products with respect to their fundamental engineering properties and performance-related characteristics.

On the basis of the demand of the available WMA additives in the industry, widely used four different Warm Mix Asphalt additives were selected named as Advera®, Cecabase RT®, Aspha-min® and Kumho. To evaluate these products Indirect Tensile Strength, Tensile Strength Ratio, Flow Number and Dynamic Modulus tests were performed in the laboratory. All results were also compared against traditional Hot Mix Asphalt.

Selection of Warm Mix Asphalt Additives

Basically, two types of additives were evaluated. One is foaming additives and the other one is Organic Additive. Later on, LeadCap, a wax type additive, was also included in the study. Advera® and Aspha-min® are the foaming additives while Cecabase RT is an organic additive.

Foaming Additives

Synthetic zeolites have been used to enhance coating of aggregates by asphalt at a lower production temperature. Zeolite includes approximately 20% of water trapped in its porous structure. Upon heating to approximately 85°C, the water is released, and then foamed asphalt is produced [6]. The zeolites are a framework of silicates that have large vacant spaces in their structures that allow space for large cations such as sodium, potassium, barium and calcium and even relatively large molecules and cation groups such as water. In the more useful zeolites, the spaces are interconnected and form long wide channels of varying sizes depending on the mineral. These channels allow the easy movement of the resident ions and molecules into and out of the zeolite structure. The most well known use for zeolites is in water softeners. Zeolites are characterized by their ability to lose and absorb water without damage to their crystal structures. They can have the water in their structures driven off by heat and other solutions pushed through the structure. They can then act as a delivery system for the new fluid.

Advera®

Advera is a product of Eurovia Services GmbH, Bottrop, Germany. It is available in a very fine white powdered form in 25 or 50 kg bags or in bulk for silos. It is a manufactured synthetic zeolite (Sodium Aluminum Silicate), which has been hydro thermally crystallized. The percentage of water held internally by the zeolite is 21 percent by mass and is released in the temperature range of 185° - 360° F. By adding Advera® to the mix at the same time as the binder, a very fine water spray is created. This release of

water creates a volume expansion of the binder that results in asphalt foam and allows increased workability and aggregate coating at lower temperatures.

According to the Manufacturer, adding Advera at a rate of 0.3 – 0.9 % percent by mass of the mix, which can result in a potential 54° F reduction in typical HMA production temperatures. This reduction in temperature is reported to lead to a 30 percent reduction in fuel energy consumption. Advera WMA manufacturer claims that a mixing temperature can be lowered by up to 21°C [34]. They state that all commonly known asphalt and polymer-modified binders can be used as well as the addition of recycled asphalt.

Aspha-min®

Aspha-min® is zeolite that is supplied in a powder or granular form and it is typically added to the asphalt mixture at a dosage of 0.3% by weight of the mix. By adding it to the mixture along with the asphalt, a very fine water spray is created as crystalline water is released, which causes a volume expansion in asphalt, thereby increasing the workability of the mixture at a lower temperature. Aspha-min® manufacturer claims that a mixing temperature can be lowered by up to 10°C [18].

Organic Additives

Organic additives, that have melting points below a normal HMA production temperature, can be added to asphalt to reduce its viscosity. With organic additives, the viscosity of asphalt is reduced at the temperature above the melting point in order to produce asphalt mixtures at lower temperatures. Below the melting point, organic additives tend to increase the stiffness of asphalt [6].

Cecabase RT®

Cecabase is an organic Additive which is liquid at 25°C used as an additive in the production of the WMA. The Cecabase RT® additive acts at the interface between mineral aggregate and asphalt, in a similar way that a surfactant acts at an interface between water and asphalt that does not significantly change the rheological properties of asphalt. CECABASE RT 945 enables to reduce the asphalt mix production and lay down temperature by 20 to 40°C and keeps the same mechanical properties as a standard HMA. The effectiveness of the Cecabase RT® was demonstrated in a field test, where a production temperature was reduced by up to 27°C yielding a WMA mixture comparable to a typical HMA mixture [14].

It is a product of Arkema Group, France and confirms that the total of 80,000 tons of warm paving materials were produced with these additives in 2007 and over 300,000 tons of WMA incorporating CECABASE RT® laid on European roads in late 2007 [13]. CECABASE RT 945 can be added either in the bitumen storage tank, or directly in line before the drum. CECABASE RT 945 is stable under the temperature of the bitumen.

CHAPTER 3 LABORATORY TEST PROCEDURE

To produce consistent specimens for laboratory testing, the same mix design para meters and testing conditions were selected for all WMA additives as well as for Hot Mix Asphalt.

Mix Design Parameters

Five stockpiles of aggregates (3/4" crushed, 3/8" chip, crushed limestone, manufactured sand, and natural sand) were blended to produce the SuperPave design gradation. Utilizing spreadsheet ability, a Superpave design gradation following graph was created as shown in Figure 1. Following the graph, 35% of the limestone, 30% of the 3/8" chip, 25% of the 3/4" crushed gravels, 5% of the manufacture sand and 5 % of the natural sand was taken in each batch. The number of gyrations required to compact the asphalt mixture were selected as 86 following the Iowa DOT specification I.M. 510, 86 for the surface mix under a traffic volume of 3 Million ESAL. The optimum asphalt (PG 70-34) content of 5.5% was selected for aggregates with a nominal maximum aggregate size of 19.0mm [16].

Dosage Rate of Warm Mix Asphalt Additives

WMA specimens were produced as per the recommendations made by manufacturer. The dosage rate and type of method for the different additives are tabulated in the Table 1. Basically, two types of the processes are used with three different additives. In the wet process, the additive is to be added with binder prior to mixing process. While in the dry process, the additive is to be added along with asphalt into the aggregate during mixing process. The specimens were prepared by wet process for

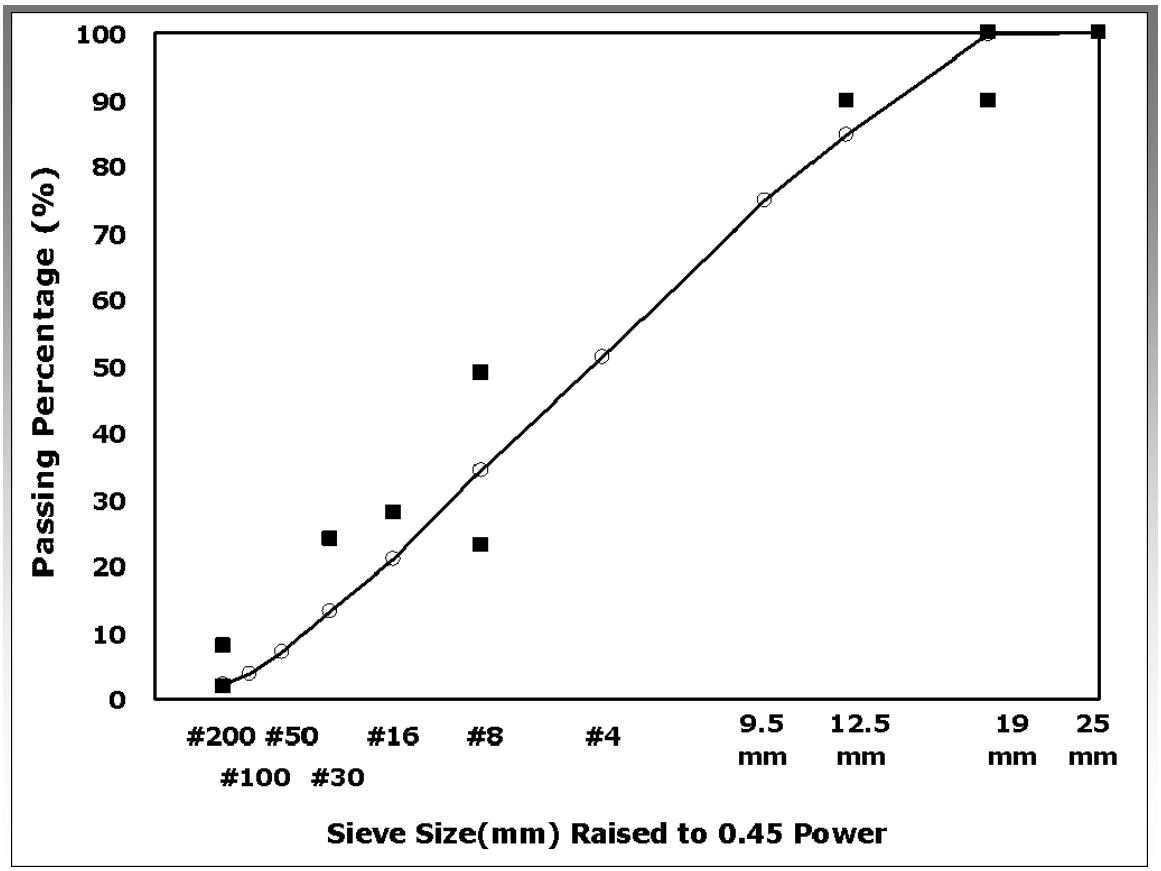

Figure 1 Design gradation used for the laboratory WMA specimens

CECABASE RT® and by a dry process for Aspha-min® (powder and granular), Advera WMA and Kumho.

Table 1Mixing process methods and quantity of WMA additive

Additive	Process	Quantity
CECABASE RT®	Wet process	0.40% of the binder weight
Aspha-min® Powder	Dry process	0.30% of the mixture weight
Aspha-min® granular	Dry process	0.30% of the mixture weight
Advera WMA	Dry process	0.25% of the mixture weight
Kumho	Dry process	1.50% of the binder weight

Sample Preparation for Warm Mix Asphalt

Following the aggregate gradation, they have been stored in different buckets. Aggregates were heated at the temperature of 125° C for 6 hours in the oven prior to mixing process. The asphalt grade PG 70-34 was selected as the binder for this study. The binder was kept in the oven for 1.5 hours at 149° C prior to mixing process. To produce WMA mixtures by the dry process, WMA additive was added to the heated aggregate and manually stirred in the bucket mixer and then asphalt was added. To produce WMA mixtures by the wet process, WMA additive was added to the heated asphalt and then added to the heated aggregate. Aggregate, asphalt and WMA additive were mixed for 60 seconds and then the WMA mixtures were heated at 125°C for 20 minutes in the oven. To compact the WMA mixtures gyratory molds were also preheated

along with the accessories at 125°C. The heated WMA mixtures at 125°C were added in a preheated gyratory mold at 125°C and compacted for 86 gyrations. All the temperatures before mixing, before compaction and after compaction were recorded. The average of all WMA and HMA Temperatures can be seen in Figure 2.

Sample Preparation for the Hot Mix Asphalt

To prepare a control HMA mixture, the aggregates were heated at a temperature of 165°C (40°C higher than the Warm Mix Asphalt Process) for 6 hours (for the same time). The same PG 70-34 asphalt was used but heated at 149°C for 1.5 hours in the oven (binder temperature same as WMA process). Then, the heated asphalt was added into the heated aggregate in the bucket mixer. Aggregate and asphalt were mixed for 60 seconds and the HMA mixtures were then heated at 135°C (15°C higher than the WMA process) for 20 minutes in the oven. To match the mixture temperature, gyratory molds were also preheated at 135°C in the oven prior to the compaction. The heated HMA mixtures at 135°C were added in a preheated gyratory mold at 135°C and compacted for 86 gyrations.

Maximum Specific Gravity

HMA and WMA mixtures were produced in the laboratory following the procedure which explained above. All the mixtures were allowed to cool at the room temperature and were stored in the refrigerator to protect the aggregate coating with the asphalt binder. Prior to an experiment, mixtures were kept in the oven at 25°C and then Maximum Specific Gravity Tests were conducted twice using the CoreLok® equipment. At first, Rice Test was conducted to find the Maximum Specific Gravity. With this

traditional test procedure proved to be ineffective in order to achieve AASHTO requirement of having the difference between the two Specific Gravity results of the same sample less than 0.5. Instead, more accurate and precise CoreLok® procedure was adopted. CoreLok® procedure [26] requires placing of the mixture in plastic bags and then the bag is to be kept inside the chamber of the CoreLok equipment. All the set points are required to be set prior to the experiment. Vacuum process automatically starts after closing the cover of the chamber. Within fraction of minutes, the sample is evacuated to 29.7 Hg and sealing of the sample is automatically been done in the chamber of the equipment. The evacuated sample is taken out and then immersed in the water to measure weight. The bag is cut from the top to allow water to go inside and subsequently fill all void spaces completely saturating the material. The sample is allowed to settle in the water and weight was measured. Weight of the bag, sample, and the combined weight of the bag and sample under water were recorded.

Bulk Specific Gravity and Air Voids

The sample was allowed to cool after compaction at room temperature for 24 hours. Then the Bulk Specific Gravity test was conducted. The bulk specific gravities of each specimen were determined following the AASHTO T 166 [1]. The water bath was filled with the water at 25±1°C (77±1.8°F) and the water level was allowed to stabilize. Three different weights, weight in the air, in the water and surface saturated weight were measured. Then, the water present on the surface of the sample was removed. The balance was reset to zero and the Surface Saturated Dry weight of the sample was recorded. Any water comes out from the specimen during this time period was counted as a weight of the saturated specimen. With the knowledge of all three weights, the bulk

specific gravities for all specimens were found using the following equation. All other calculations are shown in the Appendix B. Percentages of air voids present in the sample were found using the basic equations and are calculated and summarized in Appendix B.

Indirect Tensile Strength

To determine the Indirect Tensile Strength of all four WMA and control HMA, three samples were produced. The samples were allowed to cure at room temperature for 24 hours and the bulk specific gravity test was performed. The air voids were also calculated. All calculation can be found in Appendix B. The samples were kept at 25°C in the oven for 2 hours prior to Indirect Tensile Test.

Moisture Sensitivity Test

To evaluate the moisture sensitivity of WMA mixtures, the modified Lottman test following AASHTO T 283 [3] was performed. Six specimens (three for dry condition and three for wet condition) for each of six WMA mixtures, and the control HMA mixture were prepared. To prepare the test specimens with 7 ± 0.5% air void, all specimens were compacted at between 6 and 20 gyrations. For dry conditioning, three specimens in a sealed pack were placed in the water bath at 25˚C for 2 hours and, for wet conditioning, three specimens saturated at between 70% and 80% were placed in a freezer at -18˚C for 16 hours and in water bath at 60˚C for 24 hours followed by conditioning in water bath at 25˚C for 2 hours.

The moisture damage in asphalt mixtures is determined as a loss of strength due to the presence of moisture in terms of a tensile strength ratio (TSR) that is defined as a ratio of the indirect tensile strength of a wet specimen over that of a dry specimen.

Dynamic Modulus Test

Two samples with 100 millimeter diameter and 150 millimeter height were produced with 86 numbers of gyrations in the gyratory compactor. Samples were kept at the room temperature for 24 hours. Bulk Specific Gravities of all the specimens were measured. Both of the samples were kept again outside at the room temperature for 24 hours and prior to experiment they were kept inside the oven at three different temperatures. Three different temperature and six different frequencies were selected to carry out the test. To minimize the damage of the specimen, the test was carried out at lowest temperature 4.4°C and then preceded to higher temperatures of 21.1°C and 37.8°C. For a given temperature, the testing began with the highest frequency of loading 25Hz and proceeded to lower frequencies of 10Hz, 5Hz, 1Hz, 0.5Hz, and 0.1Hz [2]. A sinusoidal axial compressive load was applied to the testing specimen while maintaining the axial strain at 100 microstrain. The test results during the last ten cycles were recorded for each frequency.

Repeated Load Test

The repeated load test was performed on all WMA mixtures, and control WMA mixture. Two specimens for each product with 100 millimeter diameter and 150 millimeter height were produced using the gyratory compactor. The samples were left at the room temperature for 24 hours. Next day, the repeated load test was carried out using the Simple Performance Testing equipment. The uniaxial compression load without confinement was applied to obtain a loading stress level of 600kPa at 45˚C. The loading stress was applied in the form of a haversine curve with a loading time of 0.1 second with

a rest period of 0.9 second in one cycle. 10,000 cycles or 5.00 % of the cumulative permanent deformation strain was set as the limit to conduct the Repeated Load Test.

CHAPTER 4 LABORATORY TEST DATA ANALYSIS AND RESULTS

Basic characteristics of laboratory WMA specimens were measured that include mixing and compaction temperature; theoretical maximum specific gravity; bulk specific gravity; and air void. To evaluate fundamental engineering properties and performance-related characteristics of laboratory WMA specimens, analysis and results of all four laboratory tests are discussed in this section.

Mixing and Compaction Temperature

The binder temperature was kept constant at 149˚C for all WMA as well as HMA samples. However, the aggregate temperature for all WMA samples was kept between 122˚C to 125˚C as shown in Figure 2**.** The temperatures of aggregate, mixture, and compacted specimen were measured throughout the sample preparation process of each specimen. As shown in Figure 2, WMA mixtures were produced at temperatures between 117˚C and 123˚C whereas the control HMA mixture at around 149˚C. WMA mixtures were compacted at temperatures between 112˚C and 123˚C whereas the control HMA mixtures were compacted at temperatures between 126˚C and 133˚C.

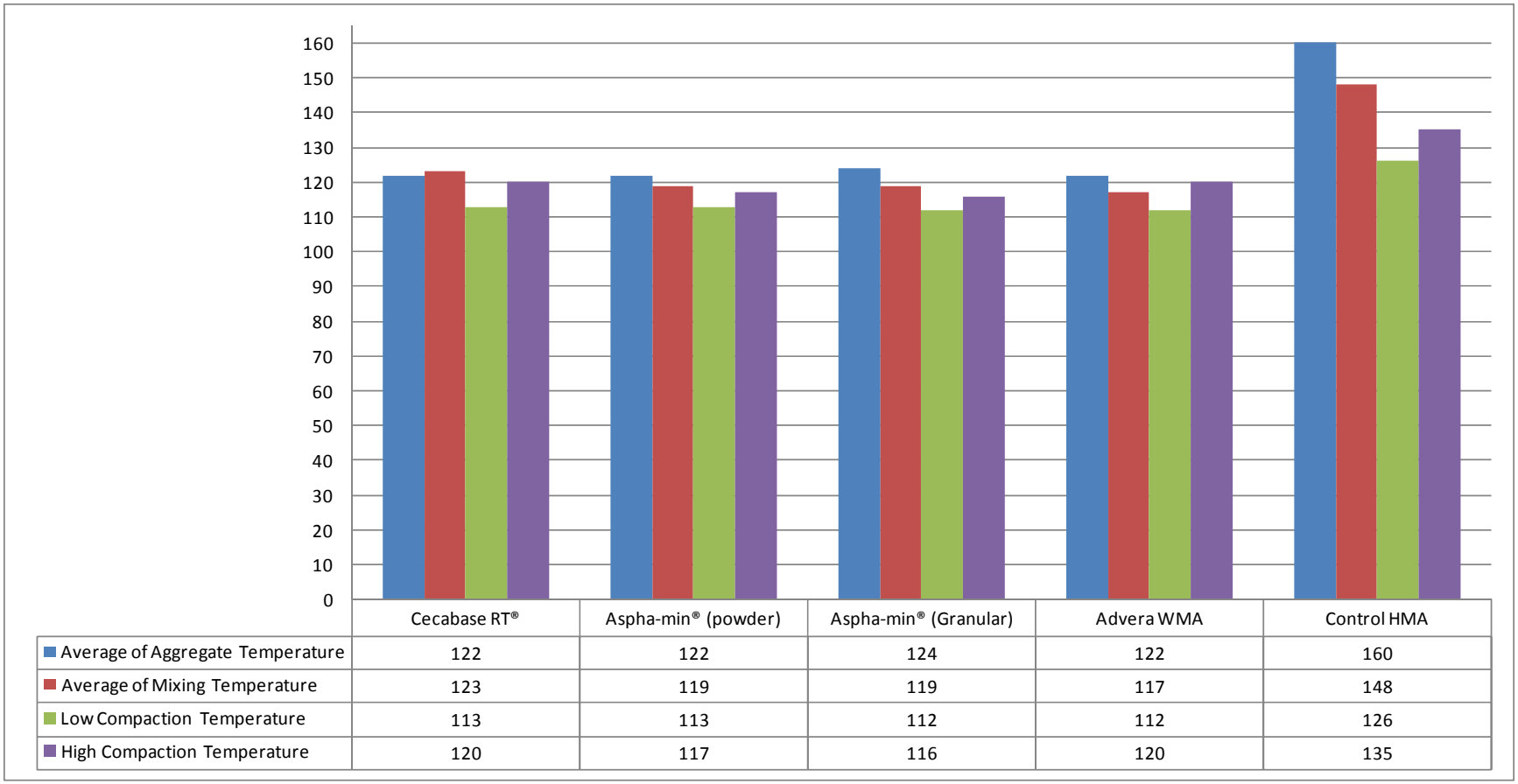

	Cecabase RT®	Aspha-min® (powder)	Aspha-min® (Granular)	Advera WMA	Control HMA
Average of Aggregate Temperature	122	122	124	122	160
Average of Mixing Temperature	123	119	119	117	148
Low Compaction Temperature	113	113	112	112	126
High Compaction Temperature	120	117	116	120	135

Figure 2 Mixing and compaction temperatures of WMA and HMA mixtures

Theoretical Maximum Specific Gravity, Bulk Specific Gravity and Air Void

The theoretical maximum specific gravity was measured twice for each mixture using a CoreLok device. It ranges between 2.420 and 2.449. Figure 3 shows the average of bulk specific gravities of three specimens prepared for the indirect tensile strength test, two specimens for dynamic modulus test, and two specimens for repeated load test with a vertical bar indicating the standard deviation for each set of specimens. Given the same compaction level of 86 gyrations, the bulk specific gravities of WMA specimens ranged between 2.362 and 2.391 and the control HMA specimens ranged between 2.372 and 2.397.

Figure 4 shows the average air voids for each set specimens with a vertical bar indicating the standard deviation. The air voids of WMA specimens ranged between 1.1% and 2.9% and the control HMA specimens ranged between 1.9% and 2.5%. As shown in Figure 4, overall, the air void of WMA specimens with granular Kumho was the lowest followed by Aspha-min® and CECABASE RT®, all of which were lower than the air void of the control HMA specimen. This result indicates these WMA additives are effective in compacting the asphalt mixture at a lower temperature.

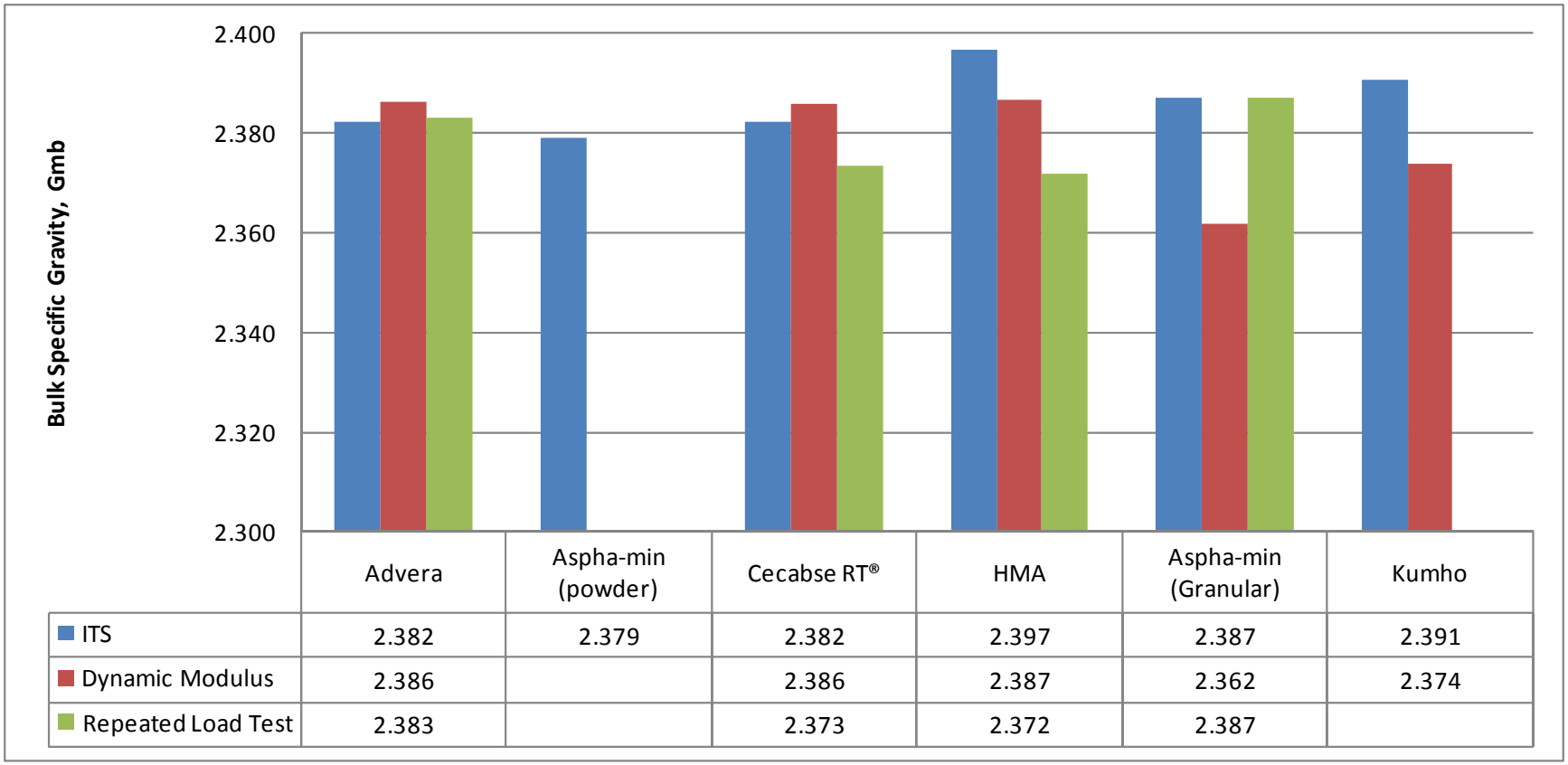

	Advera	Aspha-min (powder)	Cecabse RT®	HMA	Aspha-min (Granular)	Kumho
ITS	2.382	2.379	2.382	2.397	2.387	2.391
Dynamic Modulus	2.386		2.386	2.387	2.362	2.374
Repeated Load Test	2.383		2.373	2.372	2.387	

Figure 3 Average bulk specific gravities of WMA and HMA mixture

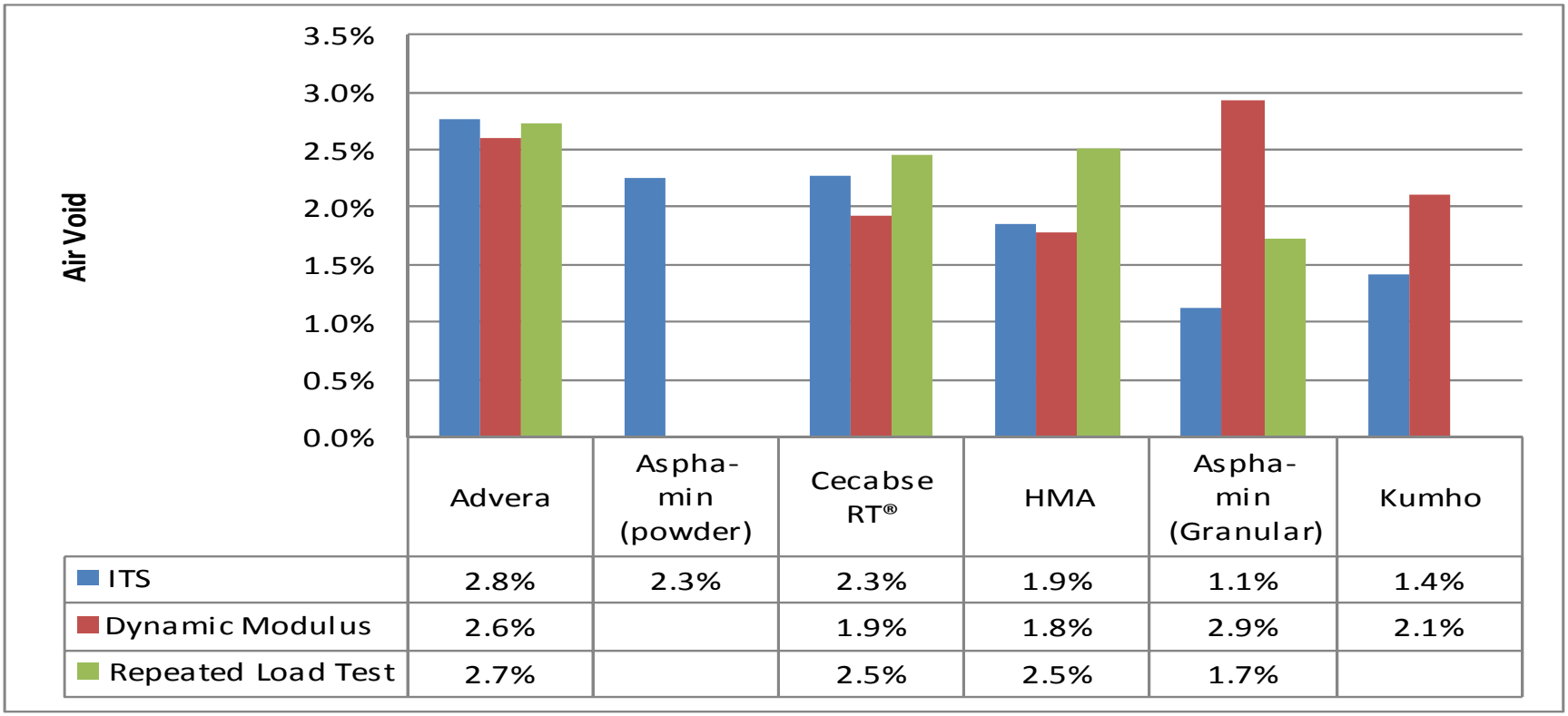

	Advera	Aspha-min (powder)	Cecabse RT®	HMA	Aspha-min (Granular)	Kumho
ITS	2.8%	2.3%	2.3%	1.9%	1.1%	1.4%
Dynamic Modulus	2.6%		1.9%	1.8%	2.9%	2.1%
Repeated Load Test	2.7%		2.5%	2.5%	1.7%	

Figure 4 Average air voids of WMA and HMA

Indirect Tensile Strength Results

Figure 5 shows the average indirect tensile strengths of six WMA mixtures, and HMA mixtures with the bar showing the standard deviation. As shown in Figure 5, the average indirect tensile strengths of WMA specimens ranged between 491kPa and 553kPa that were lower than the average indirect tensile strength (694kPa) of the HMA specimens. Therefore, the powder type of Aspha-min was not considered for the Dynamic Modulus and Repeated Load testing.

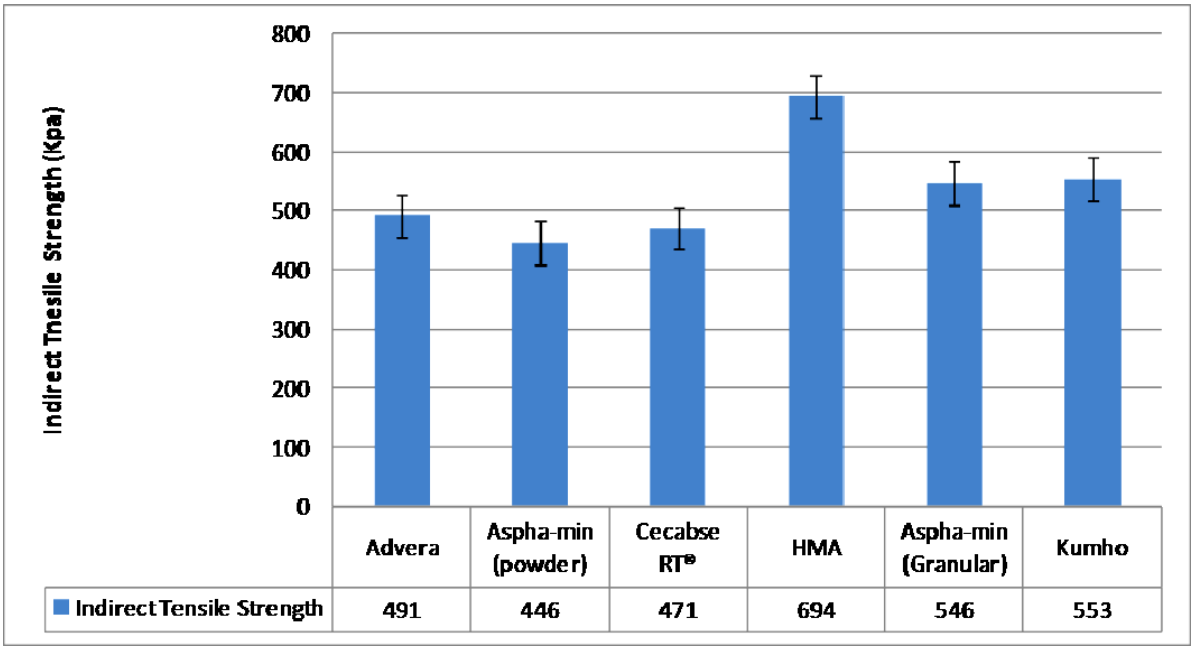

Figure 5 Average indirect tensile strengths of WMA and HMA mixtures

To determine if there is a correlation between air voids and indirect tensile strengths, as shown in Table 2, specimens were ranked in an increasing order of air voids and in a decreasing order of indirect tensile strength. Overall, WMA mixtures with the

low air voids (Aspha-min® (granular) and Kumho) exhibited the high indirect tensile strength whereas the WMA mixtures with high air voids (CECABASE RT®, Aspha-min® (powder) and Advera WMA) exhibited lower indirect tensile strength. However, the indirect tensile strength of the HMA is the highest amongst all with 1.9% air voids.

Table 2 Ranking of air voids and indirect tensile strengths of all WMA and HMA samples

Type of Mix	Ranking			
	Air void (%)	Ranking of air void	Indirect Tensile Strength (Kpa)	Ranking of ITS
CECABASE RT®	2.3%	4	471	5
Aspha-min® (powder)	2.3%	4	446	6
Aspha-min® (granular)	1.1%	1	546	3
Advera WMA	2.8%	5	491	4
Kumho	1.4%	2	553	2
Control HMA	1.9%	3	694	1

Moisture Sensitivity Test Results

Figure 6 shows average indirect tensile strengths of dry and wet conditioned samples with the bar showing the standard deviation. The TSR values of all WMA samples and the control HMA samples are labeled. As can be seen from Figure 6, the average TSR values of WMA specimens ranged between 31.9% and 61.5% whereas that of the HMA specimens was 68.0%, all below the Superpave specification of 80%. This result indicates that both HMA and WMA mixtures are susceptible to moisture damage. Particularly, the WMA mixtures with Aspha-min®, Advera WMA lost their indirect tensile strengths significantly after conditioning resulting in the lowest TSR values.

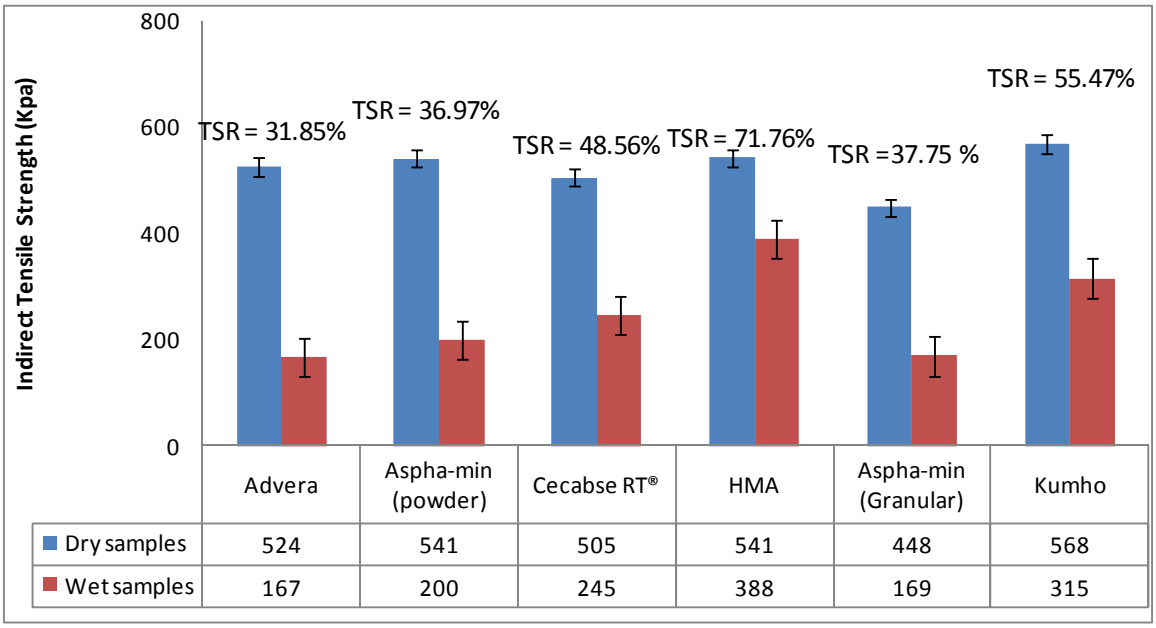

Figure 6 Average indirect tensile strengths of all samples in dry and wet conditions and tensile strength ratio of WMA and HMA mixtures

Dynamic Modulus Test Results

The average dynamic modulus of two specimens are plotted against the loading frequency at 4.4°C, 21.1°C, and 37.8°C in Figures 7 (a), (b) and (c), respectively. As shown in Figure 7 (a), at 4.4˚C, dynamic modulus of all WMA mixtures was lower than that of the control HMA mixtures. As shown in Figure 7 (b) at 21.1˚C, dynamic modulus of WMA mixtures with additives Aspha-min® (powder and granular), and Kumho, CECABASE RT® were almost similar to the control HMA mixture. The behavior of all the WMA and HMA samples at both 4.4˚C as well as 21.1˚C were found to be similar at slightly varying strength. The sudden rise in dynamic modulus of Advera WMA near 8 to 10 Hz of loading frequency shows the frequency fluctuation of the simple performance testing machine. As shown in Figure 7 (c), at 37.8˚C, dynamic moduli of WMA mixture with CECABASE RT® were higher than that of the control HMA mixture whereas the Aspha-min® exhibited the lower dynamic modulus.

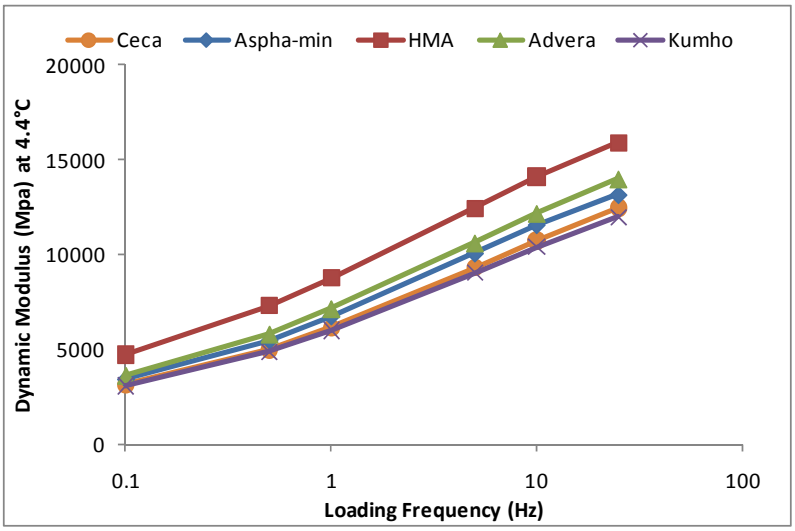

Figure 7 Average dynamic modulus of all WMA and HMA samples at 4.4°C

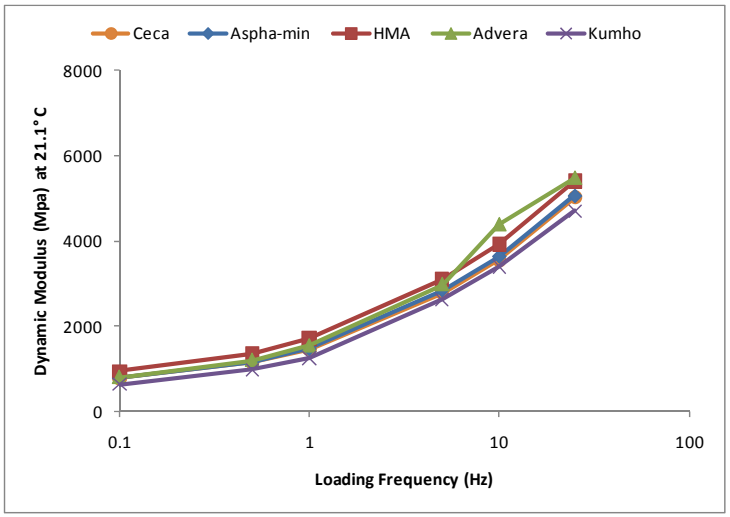

Figure 8 Average dynamic modulus of all WMA and HMA samples at 21.1°C

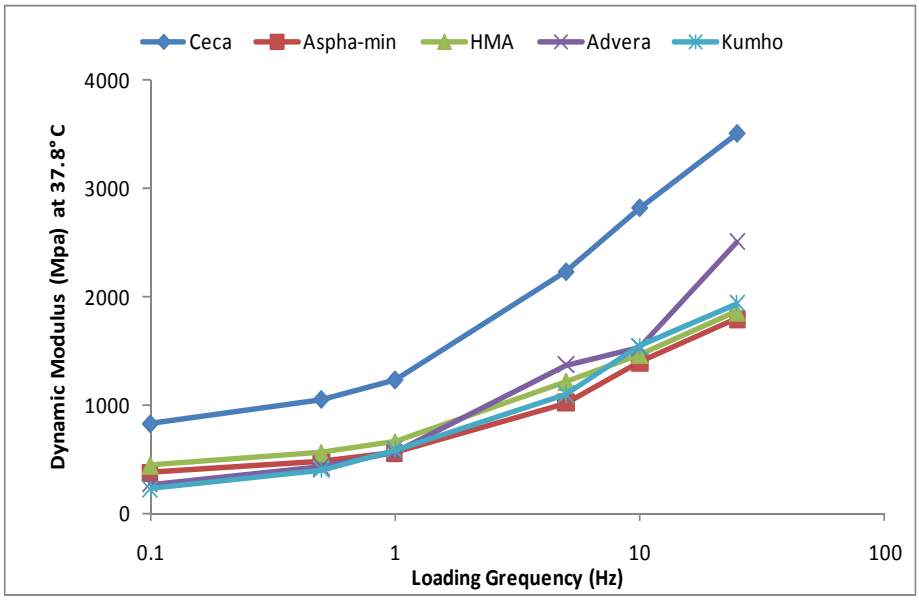

Figure 9Average dynamic modulus of all WMA and HMA samples at 37.8°C

By shifting dynamic modulus test results to a reference temperature of 21.1˚C, as shown in Figure 9, master curves were constructed for five WMA mixtures, and the control HMA mixture. Master curves of all WMA mixtures, except the one with Advera WMA, are quite similar to the control HMA mixture, which confirms that their viscoelastic responses are similar to that of HMA mixture.

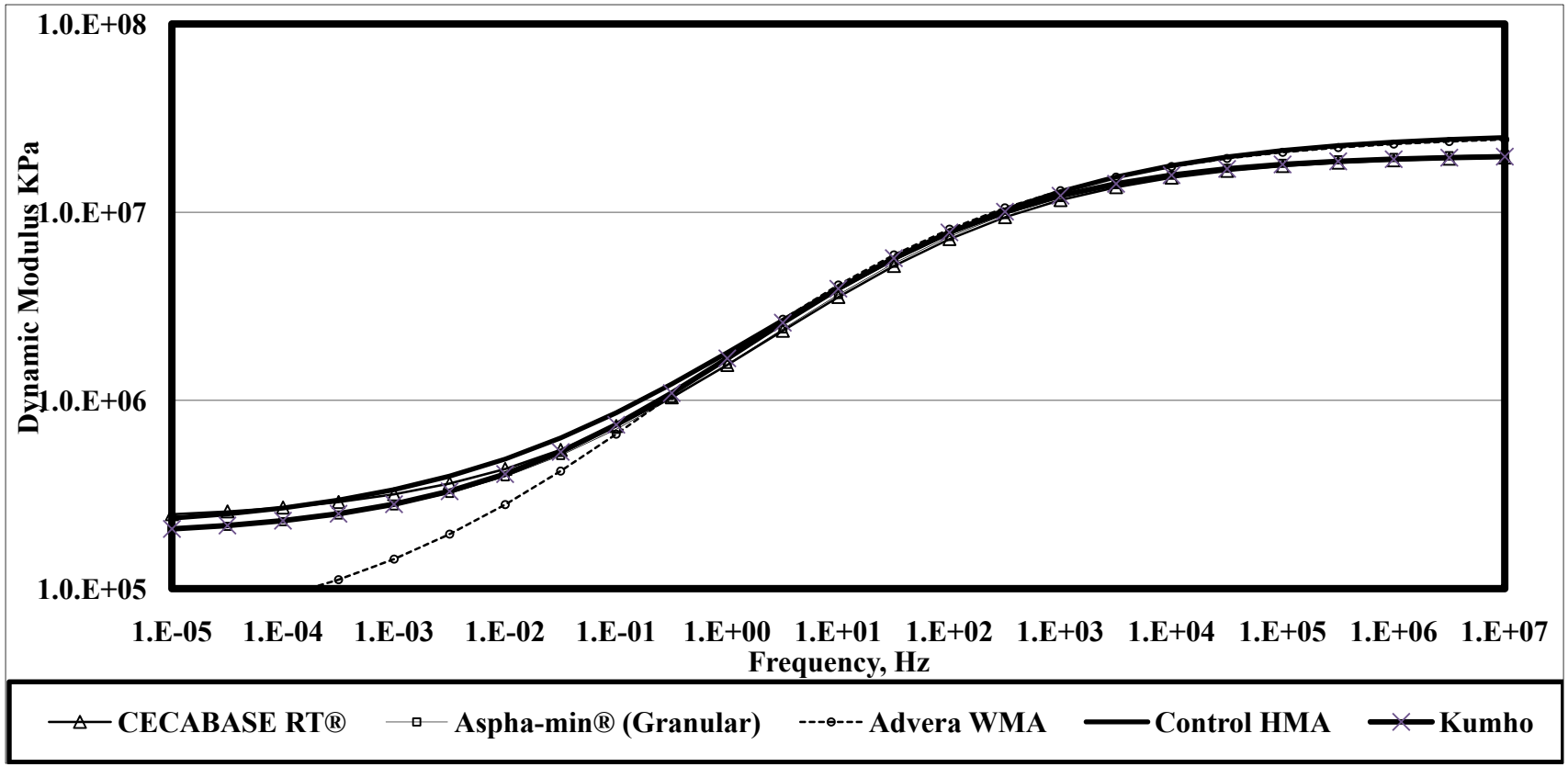

Figure 10 Master Curves of WMA and HMA Mixture

Repeated Load Test Results

WMA samples with the diameter of 100 millimeter and height of 150 millimeter were required to be produced. As per the specification, height of the specimen cannot exceed more than ±2.5 millimeters. An optimum amount of the mixture was required to be evaluated. Therefore, dummy samples of all the products were produced. Theoretical volume of the specimen was calculated. With the trial and error method, amount of mixture required to compact the mixture within the range was determined. All the weights, bulk specific gravity and volume of the samples are tabulated in the Table 3.

Figure 9 shows plots of the cumulative permanent strains against the number of loading cycles for all WMA mixtures and the control HMA mixture. Two specimens for all WMA and HMA were tested and permanent deformation was measured at each cycle.

The chart of permanent deformation was plotted against number of loading cycles. Out of all the samples produced to find the optimum amount, granular Asphamin® samples could be able utilized for repeated load test and more significantly, four samples were tested to support the significance of the results.

From Figure 9, we can see that out of all WMA samples, except granular Asphamin®, all failed to pass the requirement of 10,000 cycles. HMA undergoes the least amount of permanent deformation amongst all.

Table 3Weight of the materials required to produce samples having height between 148.5 to 152.5 millimeters

Product	Bulk specific gravity, Gmb	Volume ($\pi/4 * D^2 * h$) D= 100 mm, H= 150 mm ±2.5 mm	Weight (grams0
CECABASE RT®	2.382	1178.10 cm^3	2806.23
Aspha-min® granular	2.403	1178.10 cm^3	2830.97
Advera WMA	2.379—2.405	1178.10 cm^3	2802.70—2833.33
Hot Mix Asphalt	2.397—2.385	1178.10 cm^3	2809.77—2823.91

To determine if there is a correlation between air voids and cumulative permanent strain, as shown in Table 4, specimens were ranked in an increasing order of air voids and a cumulative permanent strain. WMA mixtures with granular Aspha-min® exhibited the lowest permanent deformation followed by the control HMA mixture whereas WMA mixtures with Advera WMA were the highest followed by CECABASE RT®.

Table 4 Ranking of air voids and permanent deformations of all the WMA and HMA samples

Type of Mix	No. of Specimen	Air Void		Ranking of Air Void	Permanent Deformation		Ranking of Permanent Deformation
		Individual	Ave.		Individual	Ave.	
CECABASE RT®	# 1	1.8%	2.1%	2	5.00%	4.63%	3
	# 2	2.5%			4.26%		
Aspha-min® (Granular)	# 1	2.2%	1.9%	1	3.28%	3.19%	2
	# 2	1.6%			3.10%		
Advera WMA	# 1	2.5%	2.6%	4	5.00%	5.00%	4
	# 2	2.6%			5.00%		
Control HMA	# 1	2.7%	2.4%	3	2.17%	2.08%	1
	# 2	2.1%			1.99%		

Overall, the specimens with higher air voids exhibited the higher permanent deformation except for the control HMA mixture that exhibited the low permanent deformation with a relatively high air void. All granular Aspha-min samples, which were almost produced with the exact similar weight and temperature resembled similarly.

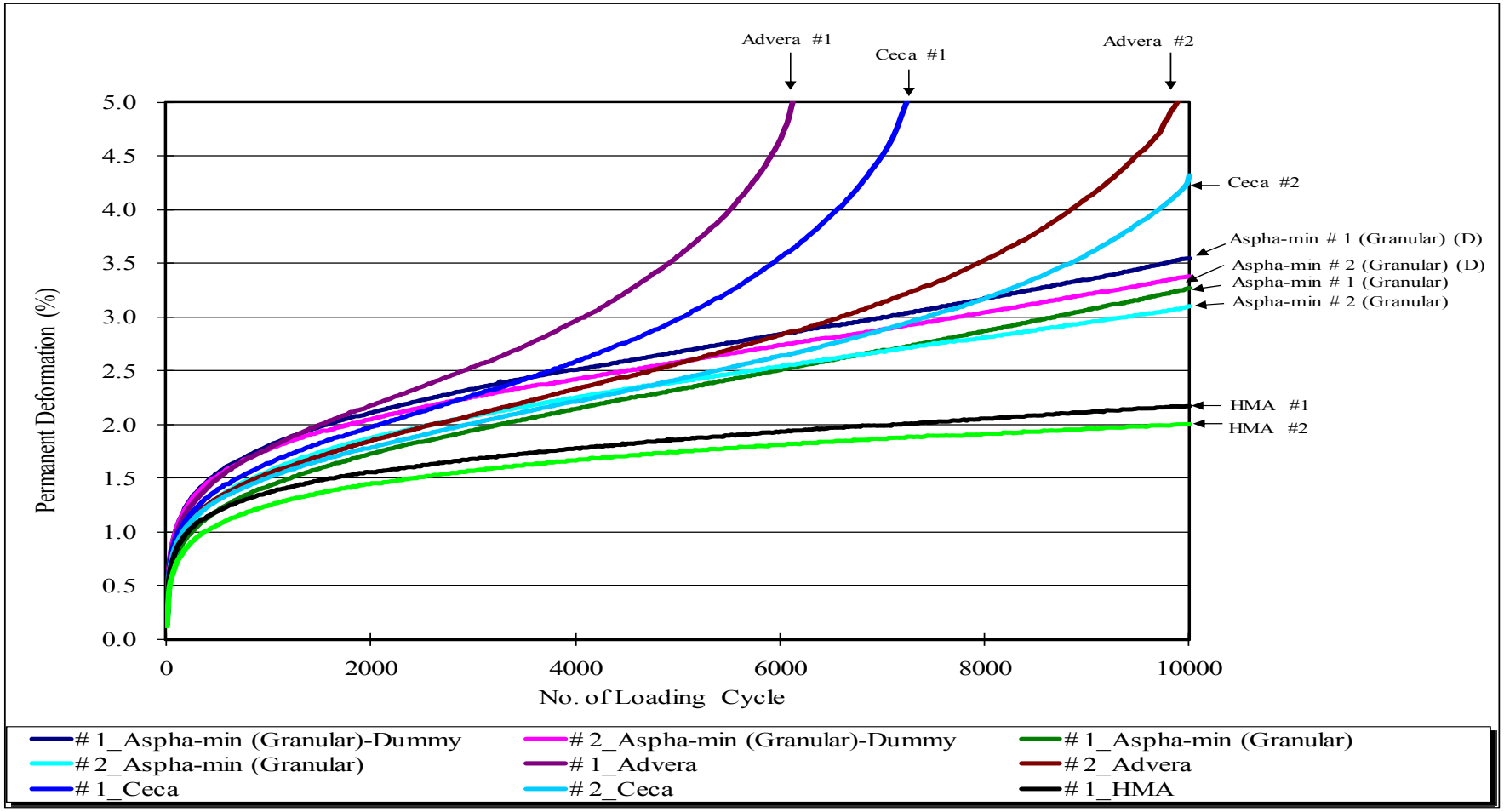

Figure 11 Plots of Permanent deformation of the WMA and HMA additives

CHAPTER 5 CHARACTERIZATION AND INTERACTION OF THE ASPHALT WITH WARM MIX ASPHALT ADDITIVES UTILIZING ATOMIC FORCE MICROSCOPY

Introduction

Right after four years of the Scanning Tunneling Microscope, Atomic Force Microscope was invented in 1986 [11]. It was examined by the observation of atomic lattice structures of graphite and sodium chloride surfaces in paraffin oil at Hansma's laboratory. The demonstration of this in-liquid observation ability of the Atomic Force Microscopy has provided greater and greater advantages to observe, analyze and find the micro level research which always proves to be an fertile asset for the asphalt industry [30].

Atomic Force Microscopy (AFM) involves the scanning of a property or surface with a cantilever. The mechanical response of the cantilever can provide the user with useful information about the sample. The information like topography would be very easy to extract. However, the images were taken beyond studying the topography and a number of images were analyzed to gain the insight knowledge of the characterization of the asphalt and interaction of the warm mix asphalt additives with asphalt. For the past few years, invention of the fast speed instruments has enabled recording capabilities of 200 images per second and has motivated the invention to be done in the area of new green asphalt technologies [8]. AFM is a relatively new instrument for imaging a sample surface which can reveal the sample surface up to nanometer size.

Literature Review

Asphalt is a complex mixture of hydrocarbons and commonly referred as colloidal systems [36]. Asphalt is usually composed of an oily phase and non-oily phase [7]. Oily phase consist of a saturated hydrocarbons (paraffinic and maltenes), cyclic products (naphthenes and aromatics) and resins (polar aromatics) while non oily phase consist of asphaltenes, carbons etc.

Ait-Kati et al. observed the asphalt using the optical microscopy and Loeber et al. and Yousefi et al. used the scanning electron microscopy (SEM). Adedeji et al. and Chen et al. tried to image the asphalt using the Transmission Electron Microscopy (TEM). The samples were prepared by dissolving Polymer Modified Asphalt intolune, putting on a cooper grid coated with formvar, and evaporating the solvent to produce a film with thickness of around 0.07μm. A preparation method in which the oil phase is leaked out by a solvent without disturbing the asphalt structure was used by Loeber et al. The de-oiled samples on the sample paper are metalized and observed with SEM. The resolution of the Scanning Electron Microscopy is very poor for the nonconducting oily samples and Loeber et al. could not find the well dispersed and aggregated forms in the image resulted compromising of the resolution capability. The resolution capability of the optical microscope is about 200 nm in best conditions while Atomic Force Microscopy gives information at atomic level [31]. In the force spectroscopy, the sample is being taken to the tip and the cantilever deflection is recorded as a function of the vertical displacement [8]. It would then be converted into force-displacement curve. However, the asphalt samples are almost liquid and very soft and it would damage the sample and contaminates surface. AFM tip and samples, ideally, never make contact to each other.

Both the TEM and SEM are high vacuum technologies and asphalt mixes tend to be somewhat oily which causes them to outgass.

Irradiation of these samples with the electron beam only makes this sort of sample more unstable. For the TEM, the sample sits in the middle of the column, with fixed and moveable apertures above and below it. Contaminants from the sample accumulate on these surfaces, seriously compromising the imaging capability of the instrument. All these pre-preparation and post preparation makes the Atomic force Microscopy as a better choice than the other microscopy. As asphalt changes its viscosity at different temperatures, Scanning Electron Microscopy, X-ray or Transmission Electron Microscopy would not suite the asphalt materials. The Atomic Force microscopy was utilized in getting number of images of asphalt and asphalt with additives as reported by The Western Research Institute [24]. The use of AFM has also been reported to directly measure the interaction between asphaltenes and silica surfaces in aqueous solutions [4].

According to Masson, The microstructural knowledge of asphalt is incomplete. There are a lot of unknown questions to be answered to understand the fundamental characteristics of the asphalt. Thirteen different types of asphalts were studied and analyzed by utilizing AFM [32]. No correlation was found between catana phase (bee structure) and asphaltene but catana phase was found to correlate well with metal contents such as vandadium and nickel. The bee structure was observed from asphalt using AFM by several researchers but no conclusion was made on its relationship with different types of asphalt [5]. Jager et al. stated that a bee structure belongs to a string-like emerging and immersing at the bitumen surface but the fact of alternating topography within a bee structure was still unanswered [37]. They reported that no

correlation was found between the type of bitumen and the topographical change. The distance between the higher parts was approximately same for all considered types of bitumen, namely 550 nm. Further, they stated that it could be explained by the arrangement of micelles but the size of the bee structure is significantly larger than typical dimensions of micelles given in the literature. One study claimed that the bee structure was correlated with the dissolution level of polymer in asphalt such that the better dissolved polymer in asphalt would exhibit less or no bee structure [28].

Atomic Force Microscopy for asphalt

The basic components of the AFM are shown in Figure 10**.** There are two major techniques to observe the surface of any sample. 1) DC or contact mode 2) AC or tapping mode. In DC mode, a tip trace a sample surface with a constant loading force and, in AC mode, a tip is vibrated vertically while scanning. To observe WMA samples, NC S15 tip was used to take images. A cantilever is attached to an actuator, commonly a tapping piezo. In response to the voltage input, the tapping piezo converts the electrical signal to an oscillatory motion that drives the base of the cantilever, causing it to oscillate in turn. For proposed research, the AC mode should be adopted in order to prevent contamination

or damage.

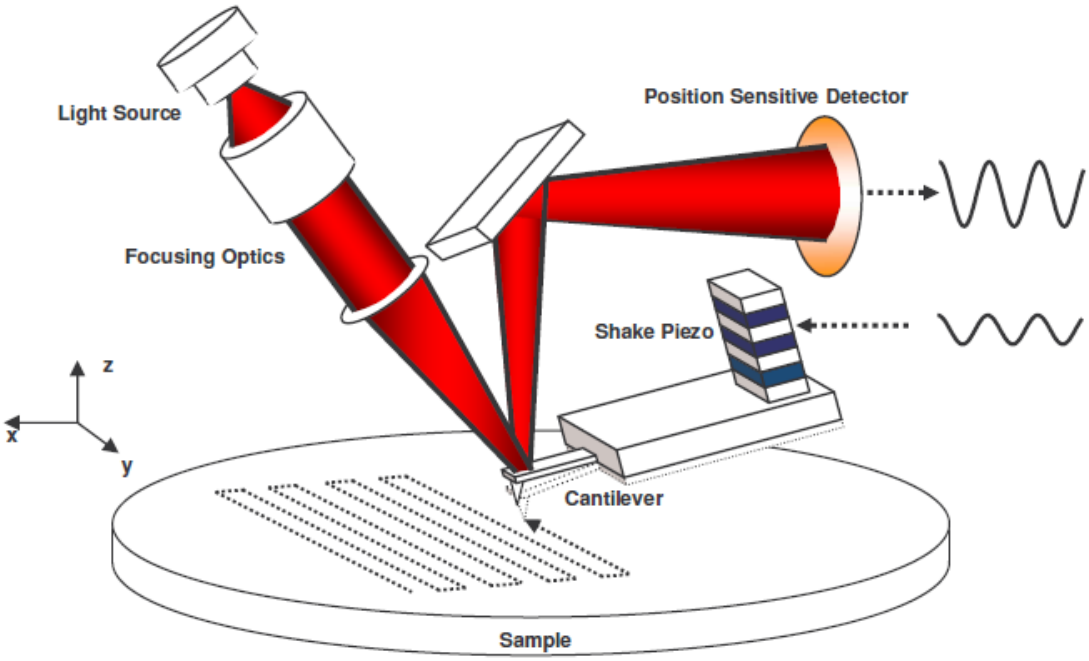

Figure 12 Basic components of Atomic Force Microscopy

Basically, an optical lever technique is used in the AFM. Light from an intense source is concentrated on flexible and reflective cantilever. The deflection of the cantilever also moves the angle of the optical beam which is transformed into an electrical signal by the position sensitive detector. As shown in the Figure 10, the sample, like a layer of asphalt, is scanned in correspondence with the cantilever in x-y plane. The AFM used for this study at the University of Iowa can be seen from Figure 11.

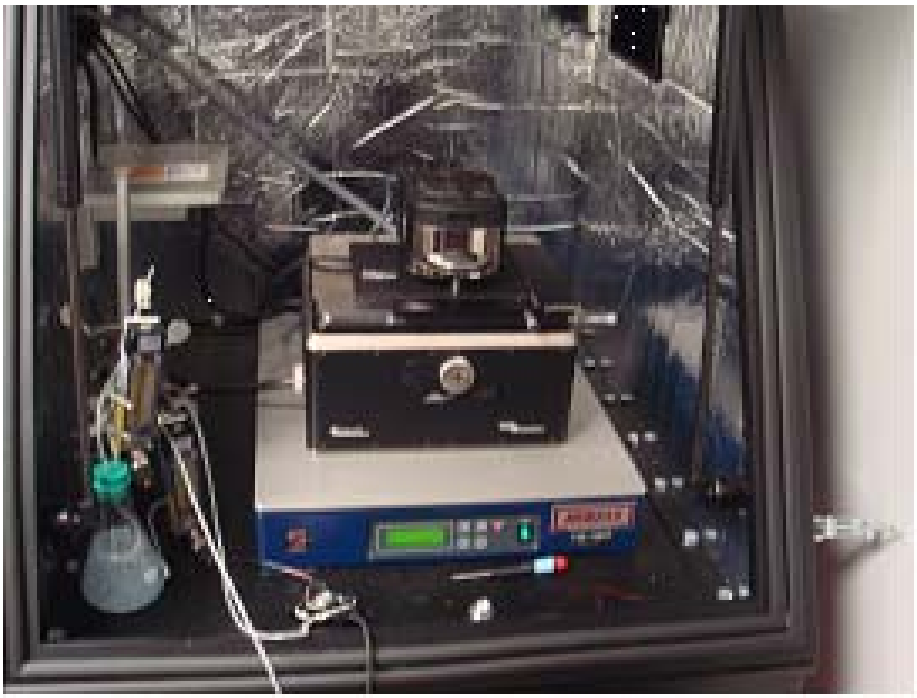

Figure 13 Atomic Force Microscopy at the University of Iowa

The Atomic Force microscopy provides information in three images as height, deflection and phase mode. When the force between tip and samples are constant, the topographic information can be recorded measured as height. While obtaining the phase information, force variations observed from scanning of the tip are recorded at constant height [27]. The deflection of the cantilever can be measured and the corresponding change of the location of the laser beam causes relocation of the photodiode array which in turn changes voltage output [15]. This change in the voltage output generates the deflection image.

Objective

The bee structures in the asphalt have been criticized by the researchers from so many years and no reason has been found yet. The literature review shows that polymer modified asphalt, and aged asphalt has some influence on the presence of the bee structures but there has been almost no research done to find the effectiveness of the WMA additives. The objective of this research is to find the effectiveness of the newly developed WMA additives in the removal of the bee structures.

Sample preparation of the WMA samples

To be easily observed by the tip, the sample is taken on a flat surface of the glass slide. Asphalt was kept in the oven at 149°C for 2 hours. The Warm Mix Additives were gradually added into the asphalt while stirring the asphalt in a container. A Number of images were taken with warm mix additives.

Test Results and discussions

As shown in the Figure 11, the bee structures can be seen in the phase image. The 3-D height image shows the exact information about the dimension of the bee structures. From Figure 11, the height of the bee structure is 40 nm and length is approximately 2 μm.

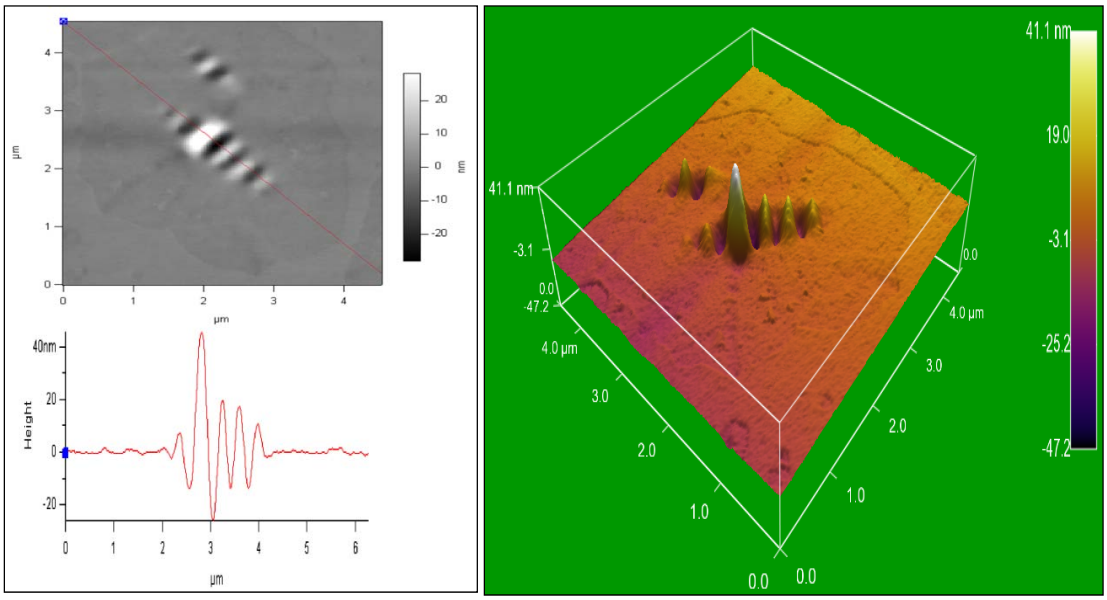

Figure 14 Phase image (left) and 3-D height image

With the Advera WMA as shown in Figure 13, the bee structures were found to be present in the asphalt and from the phase variation we can conclude that Advera WMA additive has higher phase angle and so higher viscosity. AFM images of Aspha-min® and CECABASE RT® was also taken. As expected, the Aspha-min® showed the similar results as Advera WMA.

To confirm the presence of the bee structures in the asphalt, image of virgin asphalt was also taken. As seen in the Figure 14, the bee structures are found present.

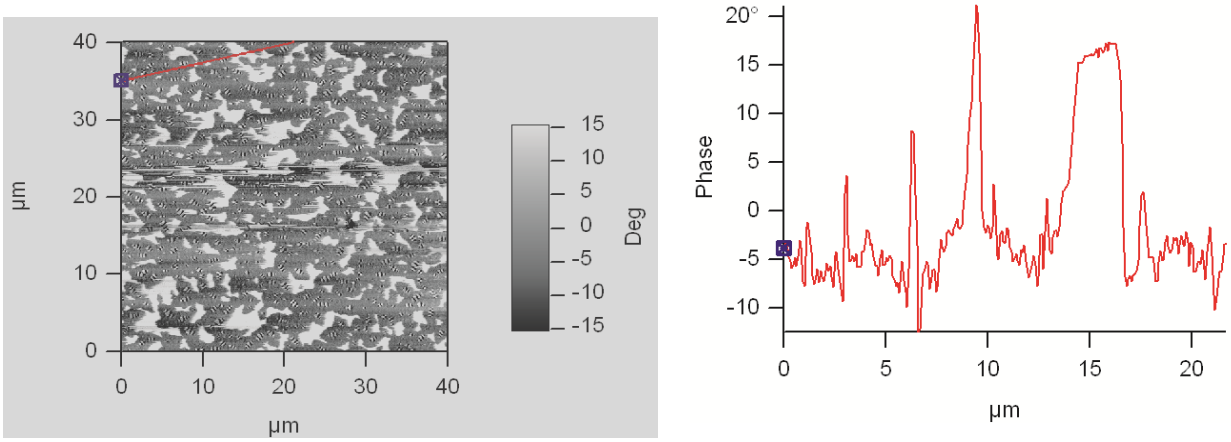

Figure 15 AFM phase image of the Advera WMA additive

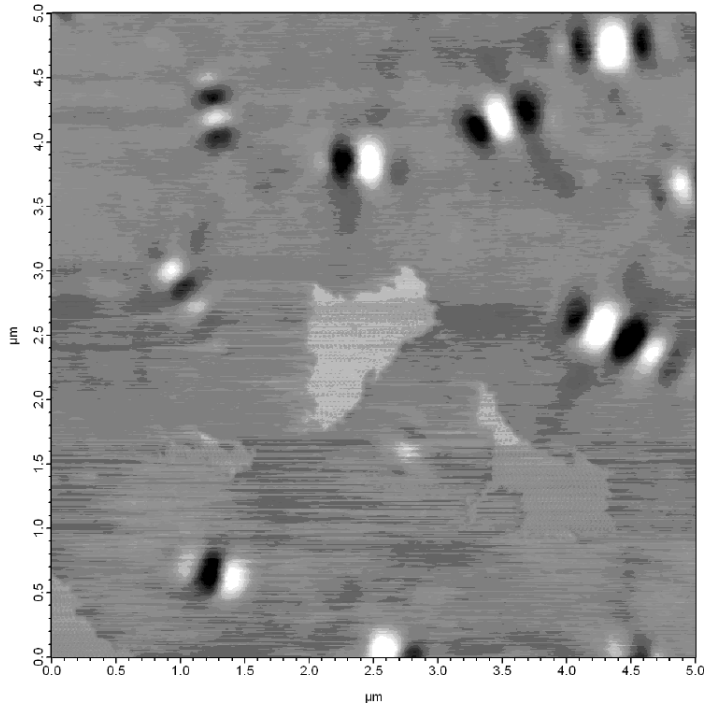

Figure 16 AFM image of Aspha-min WMA additive

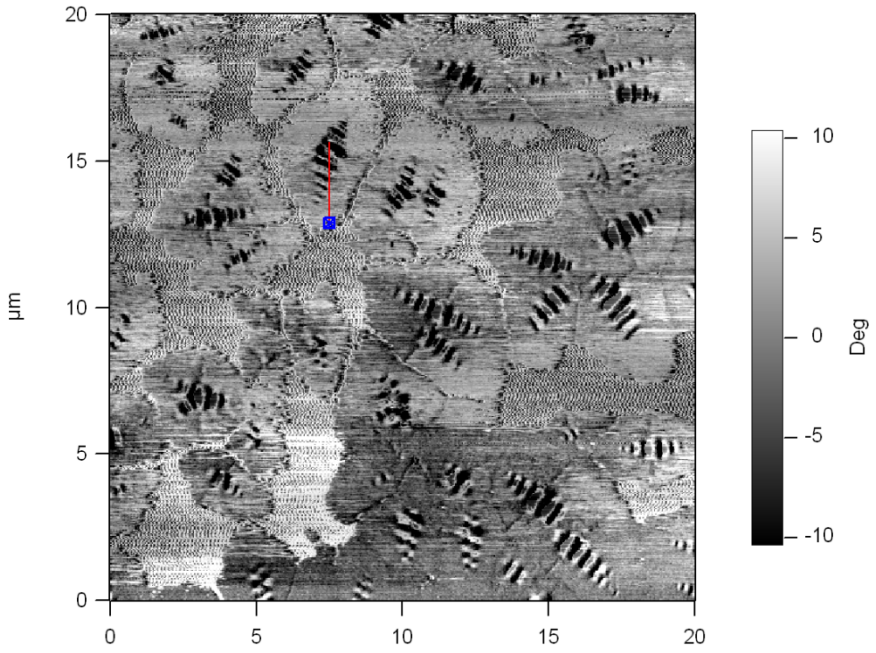

Figure 17AFM image of asphalt

The height image information with CECABASE RT® can be seen from the Figure 15. In all the images, the white colored white circles are the CECABASE RT®. It is clearly higher height, by around 40 nm, than the rest of the materials around.

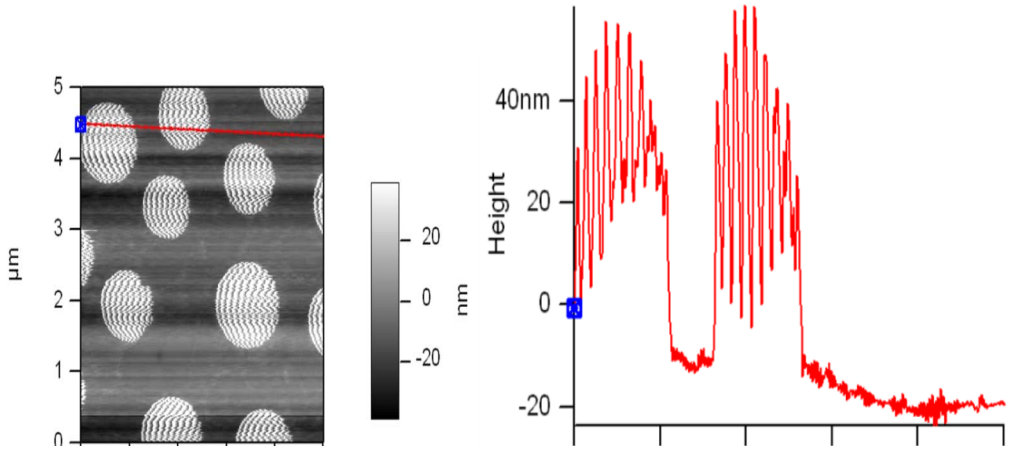

Figure 18AFM height image with CECABASE RT®

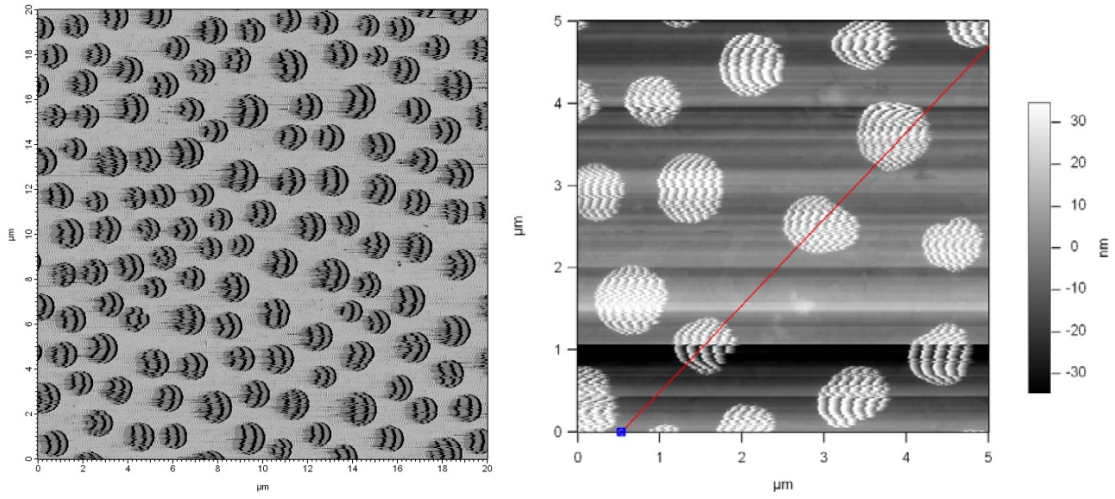

Figure 19 Disappeared bee structures with CECABASE RT

Very interestingly, while imaging with this warm mix additive with asphalt, the bee structures were found to be disappeared as can be seen from the figures shown above.

Based on this observation, CECABASE RT® seemed to have contributed in the removal of bee structures. However, to effectively prove it, more images are needed. Herein, as shown in the Figure 17**,** both CECABASE RT® and bee structures co-existed.

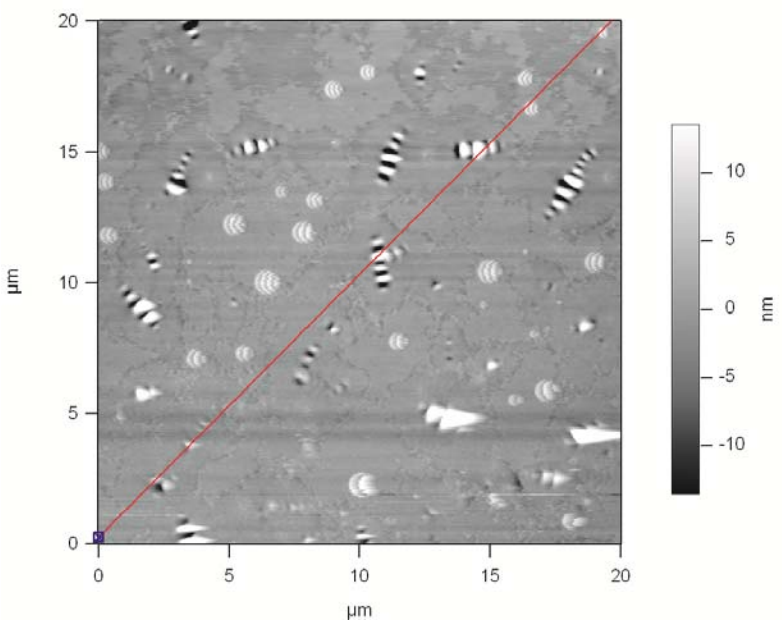

Figure 20 Bee structures seen in asphalt with CECABASE RT

From the image, it can seen that the round droplet type particles, CECABASE RT®, has a high phase angle, and they are highly viscous. As shown in Figure 18, the phase angles are plotted along the diagonal line shown in the image. From 0 to 5 nm, there are no bee structures or CECABASE RT ® droplet which is asphalt. From the image, it can be seen that asphalt has lesser phase angle and so less viscosity than the rest of the material. The drop in phase angles is due to the less viscous asphalt properties of the asphalt.

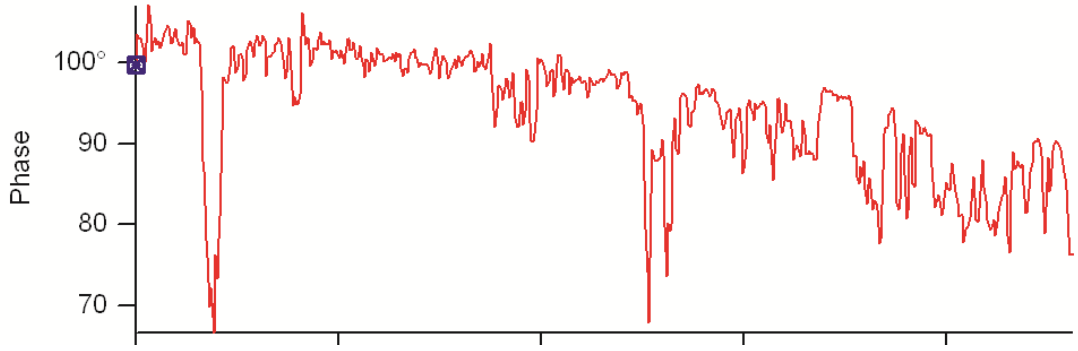

Figure 21 Phase image information of the asphalt with CECABASE RT

CHAPTER 6 SUMMARY AND CONCLUSIONS

Summary and conclusion of laboratory experiments

Warm mix asphalt (WMA) mixtures with four commercially available WMA additives, that include CECABASE RT®, Asphalt-min®, Advera WMA, Kumho, and the control HMA mixture, were evaluated for their fundamental characteristics such as air void, indirect tensile strength and moisture susceptibility. To predict a long-term performance, the dynamic modulus and the repeated load tests were conducted for all WMA mixtures as well as HMA mixtures, to make a comparison, using the simple performance testing equipment.

Rankings of Laboratory Test Results

As shown in Figure 5, WMA and HMA were ranked in terms of indirect tensile strength, tensile strength ratio, dynamic modulus and permanent deformation to make a comparison amongst them. Based on the limited test results, granular Aspha-min® and Kumho additives were effective in producing WMA mixtures in the laboratory that is comparable to HMA mixtures.

Table 5 Ranking of ITS, TSR, dynamic modulus, and permanent deformation for eight WMA mixtures and control WMA and HMA mixtures

Type of Mix	Ranking				Total average	Overall ranking
	Indirect Tensile Strength	Tensile Strength Ratio	Dynamic Modulus	Permanent Deformation		
CECABASE RT®	5	3	4	3	3.75	4
Aspha-min® (Granular)	3	4	3	2	3.00	3
Advera WMA	4	6	2	4	4.00	5
Control HMA	1	1	1	1	1.00	1
Aspha-min® (powder)	6	5	-	-	5.50	6
Kumho	2	2	-	-	2.00	2

The air void of WMA specimens with granular Kumho was the lowest followed by Aspha-min® and CECABASE RT®, all of which were lower than the air void of the control HMA specimen. Overall, the WMA mixtures exhibited similar air voids as HMA mixture which indicates these WMA additives are effective in compacting asphalt mixtures at a lower temperature.

The indirect tensile strengths of WMA specimens were lower than that of the HMA specimens except Granular Aspha-min® and Kumho. WMA mixtures with

CECABASE RT®, Advera WMA and Aspha-min® powder form showed significantly lower strength with the comparison to HMA and other WMA products. The tensile strength ratio (TSR) values of WMA mixtures and HMA mixture were below the Superpave specification of 80%. This result indicates that both HMA and WMA mixtures are susceptible to moisture damage. Particularly, the WMA mixtures with Aspha-min®, and Advera WMA lost their indirect tensile strengths significantly after conditioning.

WMA mixtures with CECABASE RT® and HMA exhibited the highest dynamic modulus. Particularly, the HMA mixture lost its dynamic modulus value more than WMA mixtures at higher test temperatures. When a test temperature was increased from 4.4˚C to 37.8˚C, CECABASE RT®, showed the highest dynamic modulus than all WMA and HMA products. This result indicates that WMA mixtures with CECABASE RT®, is less temperature sensitive than the HMA mixtures.

The WMA specimens, except CECABASE RT® and Advera WMA, passed the requirement of 10,000 cycles of repeated loading. Particularly, only the HMA mixture exhibited the lowest permanent deformation followed by the granular Aspha-min® WMA whereas WMA mixtures with Advera WMA exhibited the highest permanent deformation followed by CECABASE RT®.

Based on the limited test results, it can be concluded that Granular Aspha-min®, additive is effective in producing WMA mixtures in the laboratory that is comparable to HMA mixtures. Based on the moisture susceptibility test, no WMA mixture satisfied the Superpave requirement of 80%. Therefore, a future research should be performed to improve the moisture susceptibility of the WMA mixtures.

From the literature review, it can be concluded that for asphalt imaging, compared to Transmission Electron Microscopy (TEM), Scanning Electron Microscopy (SEM), X-ray Microscopy, AFM is the most suitable tool to adopt. Based on the three images observed of asphalt with CECABASE RT ®, bee structures could be removed from the asphalt. However, more research is needed to effectively prove the removal of the bee structures with the CECABASE RT ® additive. More images with different temperature and mixing time could give more information about the interaction of the different components of the asphalt.

APPENDIX A LABORATORY TEST PROCEDURES

All the test procedures using which the experiments were run are explained in detail below.

Maximum Specific Gravity Test

1. 3000 grams of mixture of each WMA and HMA products were made separately. The mixtures were allowed to cool at room temperature.
2. When the mixture reached around warmer temperature, all the course particles were separated into finer particles, without fracturing them, until they reached ¼ inch (6.3 mm) by hand.
3. The mixture was stored in the refrigerator.
4. 1500 grams of sample was taken for each experiment and two experiments were run for each product.
5. The mixture was first kept at the 25°C in the oven for 2 hours.
6. The weight of the CoreLok® puncture resistance bags were measured and then the mixture taken into the CoreLok® (see Figure 18) puncture resistant bags for the experiment.
7. The bag was placed inside the equipment and the sample was evacuated to 29.7 Hg and the bad was automatically been sealed.
8. After the evacuation, the bag was immersed in the water and cut from the top, while keeping the sample inside the water.

Figure A1 CoreLok equipment

9. Once, all the air voids were completely filled by water (complete saturation), the bag was allowed to settled and the weight of the bad was measured.
10. With all three weights, weight of the bag, mixture and saturated weight under the water were used in calculating the Maximum Specific Gravity.

Rice Specific Gravity Test

1. Weigh out approximately 2000 grams of asphalt mix and allow it to cool in a pan to a temperature of 25°C. Record the precise weight of the mix as *WHMA*. Using a spatula, chop up any large clumps of your mix, trying to get all of the coated aggregate specimens as separated as is possible in a few minutes time. Allow the mix to cool 20-30 minutes.
2. Fill the container until it is overflowing. Place the lid on and push it down firmly. Dry the outside of the container, and then measure its mass, ***D***. Empty all but about ¼ of the water from the container.
3. Place the ~2000 grams of asphalt mix into container. The container should be about half full.

4. Place the lid back onto the container and set it into the vibration harness and set the vibration level between 9 and 10. Pull a vacuum of 30 mmHg (using the dial on the gauge to keep it constant) on the contents for approximately 15 minutes. (Here, the objective is to remove trapped air from the submerged mix.).

Figure A2 Rice specific gravity test equipment

5. Fill the container to overflowing and press the lid down firmly. Dry the outside of the container and then re-weigh, ***E***.
6. Compute the Rice specific gravity G_{mm} of the mix as follows:

Equation 1Specific Gravity, Gmm

$$G_{mm} = \frac{W_{HMA}}{D - E + W_{HMA}}$$

Bulk Specific Gravity

1. The water bath was filled with the water at 25±1°C (77±1.8°F) and the water level was allowed to stabilize.
2. Three different weights as listed below were taken by utilizing the weighing machine.

    a. Weight in the air (W_a)

    The weight of the dry sample was taken by simply using the scale.

Figure A3 Weight of the sample in dry condition

    b. Weight in the water (W_w)

    After taking the weight in the air, the sample was kept in the water bath for 2±0.5 minutes and the weight was recorded to the nearest of 0.1 gram.

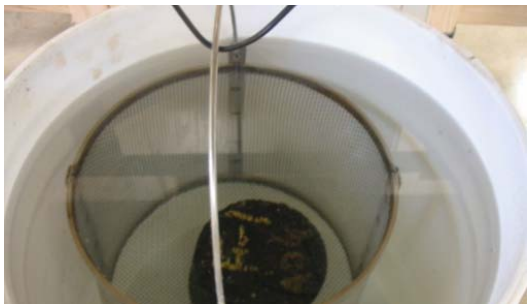

Figure A4 Weight of the sample in the water

c. Weight after removing the surface water (W_{ssd})

The sample was then removed from the water bath and the surfaces of the samples were dried with the napkin. The balance was reset to zero and very quickly, the Surface Saturated Dry weight of the sample was recorded. Any water comes out from the specimen during this time period was counted as a weight of the saturated specimen.

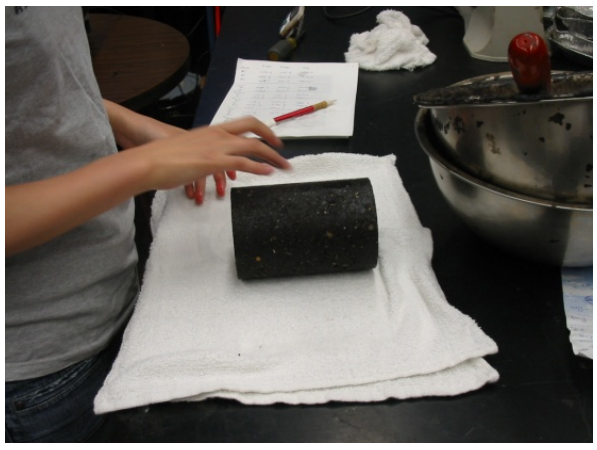

Figure A5 Surface saturation of the sample

With the knowledge of all three weights, the bulk specific gravity for all specimens were found using the following equation. All other calculations are shown in the Appendix B.

Equation 2 Bulk Specific Gravity, Gmb

$$G_{mb} = \frac{(\text{weight in air})}{(\text{SSD weight}) - (\text{submerged weight})}$$

Percentages of air voids present in the sample were found using the equation mentioned above.

Indirect Tensile Strength

1. The WMA and HMA samples were produced as mentioned in the sample preparation method in chapter 1. Partial displays of the materials are displayed in Figure 2.
2. The samples were compacted in gyratory compactor (see Figure) and the heights of all the samples were recorded. The heights of all the samples were recorded after the compaction of each sample.
3. All the samples were kept at room temperature for 24 hours in order to allow the samples to reach 25±5°C (77±9°F). The Bulk Specific Gravity test was performed following the test procedure as mentioned before.

Figure A6 Partial display of the materials used

Figure A7 Mixing equipment

Figure A8 Gyratory compactor

4. After measuring Bulk Specific Gravity, the samples were again kept at room temperature for 24 hours.
5. Then the samples were kept at 25±5°C (77±9°F) for 2 hours. Marshall Stability test was performed to measure the Indirect Tensile Strength of all the specimens. All the results and calculations can be seen in the appendix.

Figure A9 Indirect Tensile Strength test

Moisture Sensitivity Test

Preparation of Compacted Specimen

1. Six to Nine samples were produced for each test, half to be tested dry and the oth er half to be tested after partial saturation and moisture conditioning with a freeze -thaw cycle. Two additional specimens for the set were prepared. These specimen s can then be used to establish compaction procedures or the vacuum saturation technique.

Figure A10 Dry and wet set of the specimen for the moisture sensitivity test

2. Specimens 100mm in diameter by 63.5 ± 2.5mm in height. The samples having h eight more or less than 63.5 ± 2.5 millimeter were not considered for the study an d discarded.

Figure A11 Specimen after compaction

3. The mixtures were prepared in batches large enough to make at least 3 specimens . Alternatively, batch was prepared large enough to just make one specimens at a

time. While preparing a multi-specimen batch, the batch was divided into single-s pecimen quantities before placing in the oven.

(a) (b)

Figure A12 (a) Mixing of the specimen (b) Cooling of mixture at room temperature for 2 hours

4. The mixture was placed in the pan having the bottom area approximately equal to 48,400 to 129,000 mm^2 and depth approximately equal to 25 millimeter. The mixt ure was allowed to cool at 2± 0.5 hours at the room temperature.
5. Then the mixture was placed in an oven at 60 ± 3°C for 16±0.5 hours for curing. The pans were placed on spacers to allow air circulation under it.
6. After curing, the mixture was placed in an oven for 2 hours ±10 minutes at the co mpaction temperature ± 3°C prior to compaction. The mixture is compacted to 7 ± 0.5 percent air voids. The optimum number of gyrations was found necessary to achieve the air voids in the range of 6.5 to 7.5 %. The void range was obtained by adjusting different number of gyrations for different products.
7. After the specimens are removed from the molds, they are stored at room tempera ture for 24±3 hours.

Evaluating and Grouping of Compacted Specimens

After curing, the following tests and measurements of each specimen were conducted by following the methods explained before:

1. The maximum specific gravity (G_{mm}) was measured using CoreLok device.
2. The thickness (t) and diameter (D) was measured of each specimen.
3. The bulk specific gravity (G_{mb}) was measured in accordance with AASHTO – T 166. The volumes of the specimens were determined by subtracting the specimen weight in water from the saturated, surface-dry weight.

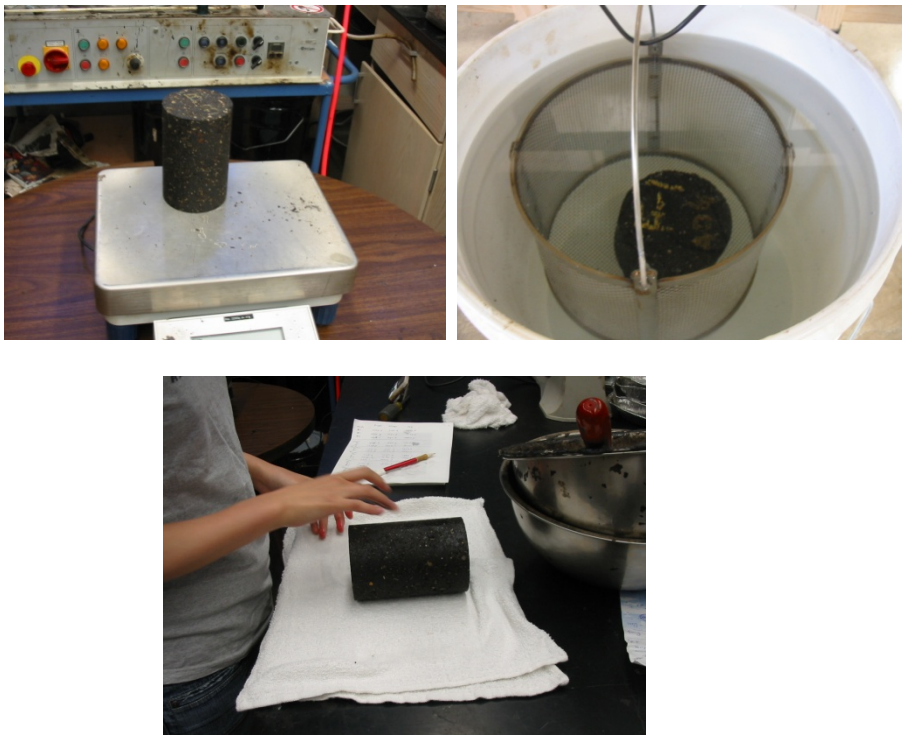

Figure A13 Bulk specific gravity test

4. Once determined, the specimens are separated into two subsets, of at least three specimens each, so that the average air voids of the two subsets, for dry subset spe

cimens and wet subset specimens, are approximately equal.

Figure A14 Determination of the dry and wet subsets of the specimen

5. If the determined air void is found out of range from 6.5% to 7.5%, the specimen was discarded.

Reconditioning of Specimens

At the end of the curing period, the dry subset was wrapped with plastic in a heavy duty, leak proof plastic bag. The specimens were then placed in a 25±0.5°C water bath for 2 hours±10 minutes with a minimum of 25mm of water above their surface.

Figure A15 Reconditioning of the samples

The wet subset is conditioned as follows:

1. The specimens were placed in a vacuum container supported a minimum of 25m m above the container bottom.
2. The container is filled with potable water at room temperature so that the specim ens have at least 25mm of water above their surface.
3. A vacuum of 250-660 mmHg partial pressure is applied for approximately 5 to 1 0 minutes depending upon vacuum system and level of air void.

Figure A16 Vacuum of the samples

4. The vacuum is removed and the specimen is left submerged in water for approxi mately 5 to 10 minutes.

Figure A17 Specimen submerged in the water after vacuuming for 5 to 10 minutes

5. Measure the weight of the saturated and surface-dry specimen after partial vacuu m saturation is done.

Figure A18 Measurement of saturated and surface dry weight of the samples

6. The degree of saturation level is determined by comparing the volume of absorbe d water with the volume of air voids using the excel sheet.
7. If the degree of saturation is between 70 and 80 percent, the conditioning by free zing may continue. If the degree of saturation is less than 70 percent, the vacuum procedure using more vacuum and/or time is repeated. If the degree of saturation is more than 80 percent, the specimen is considered damaged and is discarded.

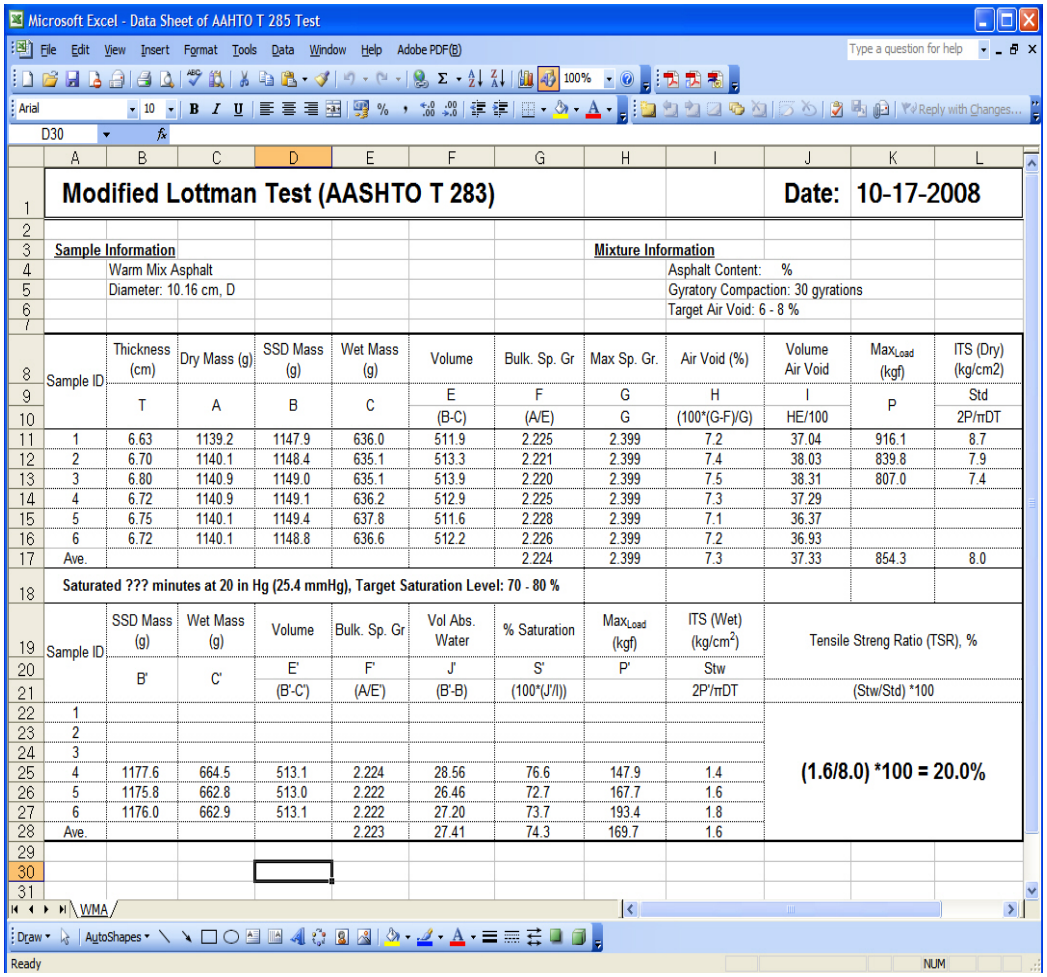

Microsoft Excel - Data Sheet of AAHTO T 285 Test

Modified Lottman Test (AASHTO T 283) — **Date: 10-17-2008**

Sample Information
Warm Mix Asphalt
Diameter: 10.16 cm, D

Mixture Information
Asphalt Content: %
Gyratory Compaction: 30 gyrations
Target Air Void: 6 - 8 %

Sample ID	Thickness (cm)	Dry Mass (g)	SSD Mass (g)	Wet Mass (g)	Volume	Bulk. Sp. Gr	Max Sp. Gr.	Air Void (%)	Volume Air Void	Max_{Load} (kgf)	ITS (Dry) (kg/cm2)
	T	A	B	C	E	F	G	H	I	P	Std
					(B-C)	(A/E)	G	(100*(G-F)/G)	HE/100		2P/πDT
1	6.63	1139.2	1147.9	636.0	511.9	2.225	2.399	7.2	37.04	916.1	8.7
2	6.70	1140.1	1148.4	635.1	513.3	2.221	2.399	7.4	38.03	839.8	7.9
3	6.80	1140.9	1149.0	635.1	513.9	2.220	2.399	7.5	38.31	807.0	7.4
4	6.72	1140.9	1149.1	636.2	512.9	2.225	2.399	7.3	37.29		
5	6.75	1140.1	1149.4	637.8	511.6	2.228	2.399	7.1	36.37		
6	6.72	1140.1	1148.8	636.6	512.2	2.226	2.399	7.2	36.93		
Ave.						2.224	2.399	7.3	37.33	854.3	8.0

Saturated ??? minutes at 20 in Hg (25.4 mmHg), Target Saturation Level: 70 - 80 %

Sample ID	SSD Mass (g)	Wet Mass (g)	Volume	Bulk. Sp. Gr	Vol Abs. Water	% Saturation	Max_{Load} (kgf)	ITS (Wet) (kg/cm^2)	Tensile Streng Ratio (TSR), %
	B'	C'	E'	F'	J'	S'	P'	Stw	
			(B'-C')	(A/E')	(B'-B)	(100*(J'/I))		2P'/πDT	(Stw/Std) *100
1									
2									
3									
4	1177.6	664.5	513.1	2.224	28.56	76.6	147.9	1.4	**(1.6/8.0) *100 = 20.0%**
5	1175.8	662.8	513.0	2.222	26.46	72.7	167.7	1.6	
6	1176.0	662.9	513.1	2.222	27.20	73.7	193.4	1.8	
Ave.				2.223	27.41	74.3	169.7	1.6	

Figure A19 Spreadsheet for the calculation of the Tensile Strength Ratio

8. For specimens with 70 to 80 percent saturation, the specimens are each wrapped with a plastic film such as saran wrap and placed in a plastic bag containing 10±0 .5 ml of water and sealed. The plastic bags are placed in a freezer at a temperatur e of -18±3°C for 16 hours± 10 minutes. Remove the specimens from freezer.

Figure A20 Freezing of the wet specimen at -18° C for 16 hours

9. Place the specimens in a water bath at 60±1°C for 24±1 hours. The specimens sh ould have a minimum of 25mm of water above their surface. As soon as the speci mens are placed in the water bath, the plastic bag and film is removed from each specimen.

Figure A21 Specimen inside the water at 60° C for 24 hours

10. After 24±1 hours in the water bath, the specimens are removed and placed in a w ater bath at 25±0.5°C for 2 hours±10 minutes. The specimens should have a mini mum of 25mm of water above their surface.

Figure A22 Dry and wet specimens inside the water at 25° C for 2 hours

11. The specimen is removed from the bath, the thickness determined, and then placed on its side between the bearing plates of the testing machine. Steel loading strips are placed between the specimen and the bearing plates. A load is applied to the specimen by forcing the bearing plates together at a constant rate of 50mm/ minute.

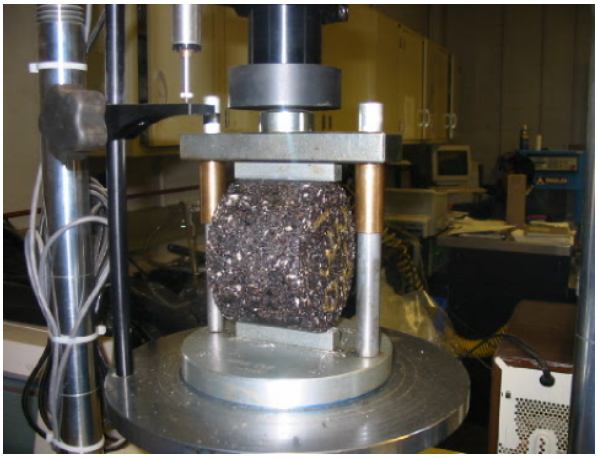

Figure A23 Indirect Tensile Strength of the specimen

12. The maximum load is recorded, and the load continued until the specimen cracks. The machine is stopped and the specimen broken apart at the crack for observation.
13. The tensile strength is calculated using the following equation:

Equation 3 Tensile Strength

$St = 2P / \pi t D$

Where:

St = tensile strength, psi

P = maximum load, lbs

t = specimen thickness, in.

D = specimen diameter, in.

14. The tensile strength ratio is calculated as follows:

Equation 4 Tensile Strength Ratio

Tensile Strength Ratio (TSR) = S_1/S_2

Where:

S_1 = average tensile strength of the dry subset, psi

S_2 = average tensile strength of the conditioned subset, psi

Repeated Load Test

Day 1

1. Prepare two batches of 6000 grams of aggregate based on gradation and put in oven overnight at 125°C for Warm mix asphalt samples and 165°C for Hot Mix Asphalt samples.

Day 2

1. Put gyratory molds and all other laboratory utensils in the oven 2 hours prior to an experiment.

2. Make asphalt mixture using mixture machine and prepared raw materials. Take temperature measurements before and after mixing.
3. Measure asphalt mixture onto pie tins and put back in oven for about 5-10 minutes to heat up and reach appropriate compaction temperature. Specimen heights must be 150mm +/- 2mm at 86 gyrations. This can be achieved with samples weighing the mixtures approximately 2780 grams.
4. After reaching compaction temperature, prepare mold with asphalt mixture and compact using gyratory compactor at 86 gyrations. Take temperature measurement before and after compaction.

Day 3

1. Measure dry weight of each specimen.
2. Measure weight of each specimen in water.
3. Measure surface saturation dry weight of each specimen.
4. Calculate the bulk specific gravity of the samples.

Day 4

1. Plug in ITC machine main cable and turn on air supply. Set temperature to 45°C as shown in Figure 24.
2. Turn on the temperature controller power switch located behind the unit as shown in Figure 26.
3. Put one dynamic creep sample into oven at 45°C for 2 hours.
4. Open the ITC software and make sure the hydraulics are turned on. (Shortcut to Unitest 21534m.exe)

5. Once the analysis of first the sample gets complete, replace with second sample and repeat the analysis.

Figure A24 ITC main supply

Figure A25 Temperature controller and the power switch of ITS

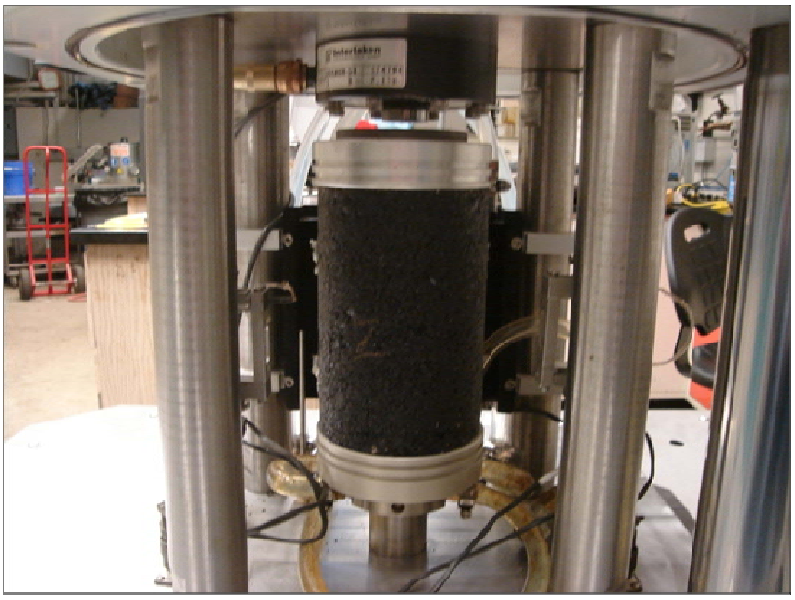

Figure A26 Placement of samples in ITS chamber

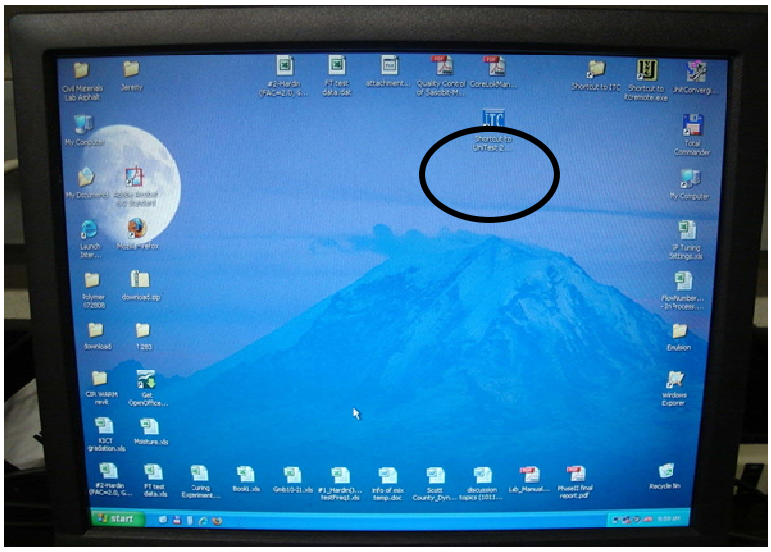

Figure A27 Shortcut to ITS software.

Dynamic Modulus Test

1. The samples were made in the same way as made for the Repeated Load test (same procedure explained before Day 4).
2. Apply four magnets on each of the two dynamic modulus samples using epoxy.
3. After epoxy has set, put samples into refrigerator overnight at 4.4° C.
4. Store some water in pan to make it in a ice form which will be used later.

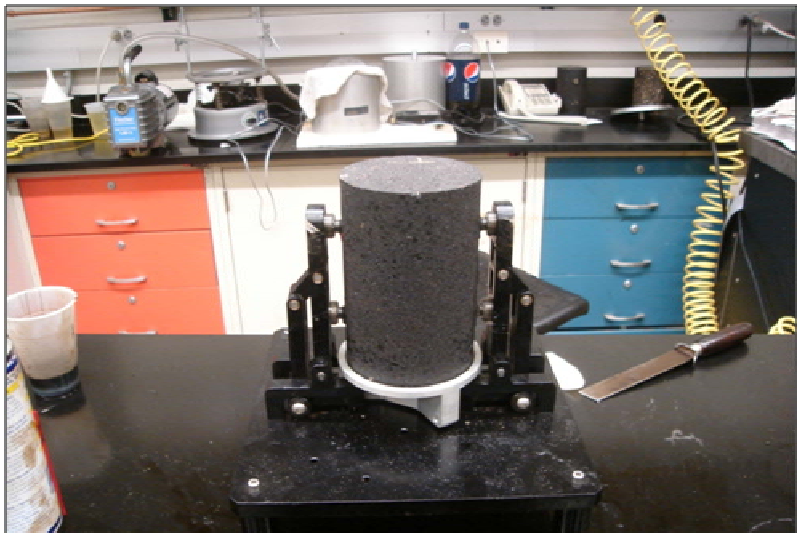

Figure A28 Application of magnets using epoxy on dynamic modulus samples

Day 5

1. Put first dynamic modulus sample into ITS machine at 4.4°C.
2. Attach sensor to the magnets and make sure that pin to the sensors is in the position and the LVDT1 and LVDT2 values in t he software are negative.
3. Apply stroke through the software which would lift the sample and make contact with the surface as shown in Figure 30.
4. After closing the lid, recheck the temperature settings.

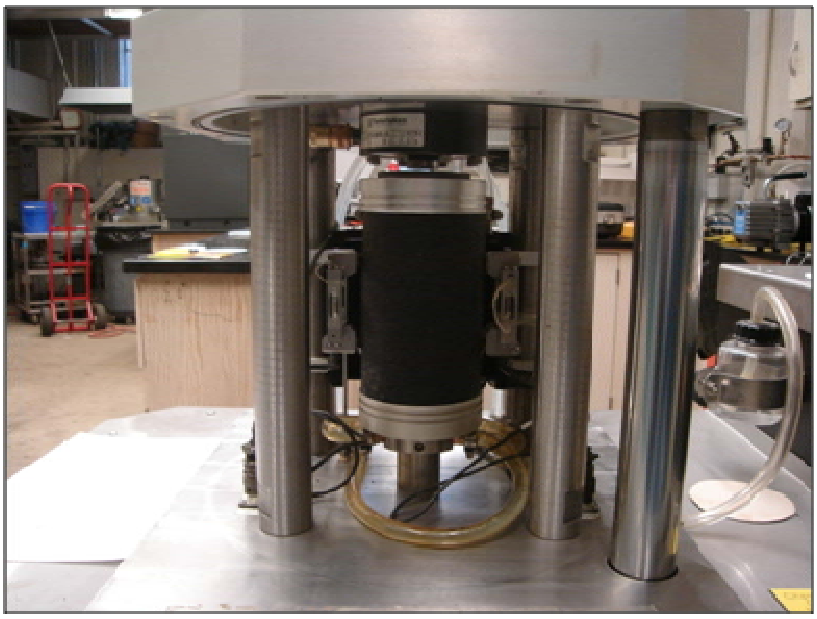

Figure A29 Position of the sample with attached sensors

Figure A30 Lifting of the sample until it touches top

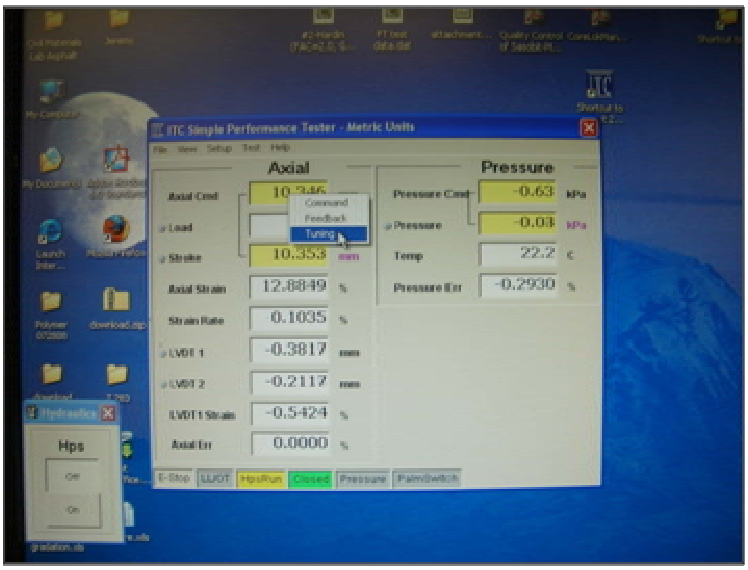

Figure A31 Selecting tuning option in the ITS software

5. In the drop down menu below Axial, select Load and enter the tuning data from the SP Tuning Settings.xls spreadsheet located on the desktop. (Low=4.4°C, Mid=21.1°C, High=38°C)
6. Once the temperature reach to setting temperature run the dynamic modulus test.
7. Repeat the same procedure for second sample.
8. Once the test is finish, put the pan of ice into the oven with the tested samples to allow them reach at the temperature 21.1°C.

Day 6

1. Set ITS machine temperature to 21.1°C.

2. Once the temperature reaches to setting temperature, put first sample into the machine and tune the settings by repeating steps 2 through 8 of Day 5 procedure.
3. After dynamic analysis has been completed for both samples, put the samples into an oven overnight at 38°C.

Day 7

1. Set ITS machine temperature to 38°C.
2. Once the temperature reaches to setting temperature, put first sample into the machine and tune the settings by repeating steps 2 through 8 of Day 5 procedure.
3. Once dynamic modulus analysis is complete, remove the magnets from the samples and clean everything with WD-40.
4. Discard the finished samples.

APPENDIX B DATA OF ALL EXPERIMENTS

Indirect Tensile Strength Results

Table B1 ITS Test results Advera WMA

Advera														
Asphalt Content (%)	**No.**	**Height (mm)**	**Weight (g)**			**Volume**	**Bulk Density**	**Theoretical Max. Density**	**Asphalt Volume (%)**	**Air Voids (%)**	**VMA (%)**	**VFA (%)**	**ITS (kg/cm^2)**	**Deformation (mm)**
			Air	**Water**	**SSD**									
A		T	B	C	D	E	F	H	I	J	K	L		
Gravity of asphalt binder, G = 0.93						D - C	B / E		(A*F) / G	(H-F) / H *100	I + J	(K-J) / K *100	(2*P) / (π*Q*T)	
5.5	1	62.8	1144.7	662.3	1146.5	484.2	2.364	2.450	13.98	3.5	17.5	80.0	4.464	1.40
	2	62.1	1148.8	670.3	1150.0	479.7	2.395	2.450	14.16	2.3	16.4	86.3	5.266	1.84
	3	62.6	1150.1	669.3	1151.0	481.7	2.388	2.450	14.12	2.5	16.7	84.7	5.298	1.67
	Ave.					481.9	2.382	2.450	14.09	2.8	16.9	83.6	5.0	1.64

Table B2 ITS Test results Aspha-min (powder form)

Aspha-min (powder type)														
Asphalt Content (%)	**No.**	**Height (mm)**	**Weight (g)**			**Volume**	**Bulk Density**	**Theoretical Max. Density**	**Asphalt Volume (%)**	**Air Voids (%)**	**VMA (%)**	**VFA (%)**	**ITS (kg/cm^2)**	**Deformation (mm)**
			Air	**Water**	**SSD**									
A		T	B	C	D	E	F	H	I	J	K	L		
Gravity of asphalt binder, G = 0.93						D - C	B / E		(A*F) / G	(H-F) / H *100	I + J	(K-J) / K *100	(2*P) / (π*Q*T)	
5.5	1	62.8	1149.8	668.4	1151.2	482.8	2.382	2.434	14.08	2.2	16.2	86.7	4.465	1.40
	2	63.8	1146.3	663.7	1148.1	484.4	2.366	2.434	14.00	2.8	16.8	83.4	4.233	1.84
	3	62.1	1145.0	666.6	1145.8	479.2	2.389	2.434	14.13	1.8	16.0	88.5	4.943	1.67
	Ave.					482.1	2.379	2.434	14.07	2.3	16.3	86.2	4.5	1.64

Table B3 ITS Test results Cecabase RT

Cecabase RT														
Asphalt Content (%)	**No.**	**Height (mm)**	**Weight (g)**			**Volume**	**Bulk Density**	**Theoretical Max. Density**	**Asphalt Volume (%)**	**Air Voids (%)**	**VMA (%)**	**VFA (%)**	**ITS (kg/cm^2)**	**Deformation (mm)**
			Air	**Water**	**SSD**									
A		T	B	C	D	E	F	H	I	J	K	L		
Gravity of asphalt binder, G = 0.93						D - C	B / E		(A*F) / G	(H-F) / H *100	I + J	(K-J) / K *100	(2*P) / (π*Q*T)	
5.5	1	61.5	1147.0	669.3	1148.2	478.9	2.395	2.438	14.16	1.8	15.9	88.9	5.069	1.40
	2	57.8	1048.7	606.5	1049.6	443.1	2.367	2.438	14.00	2.9	16.9	82.7	4.504	1.84
	3	62.1	1135.7	660.5	1136.6	476.1	2.385	2.438	14.11	2.2	16.3	86.7	4.823	1.67
	Ave.					466.0	2.382	2.438	14.09	2.3	16.4	86.1	4.8	1.64

Table B4 ITS Test results Aspha-min (granular)

Aspha-min (granular)														
Asphalt Content (%)	**No.**	**Height (mm)**	**Weight (g)**			**Volume**	**Bulk Density**	**Theoretical Max. Density**	**Asphalt Volume (%)**	**Air Voids (%)**	**VMA (%)**	**VFA (%)**	**ITS (kg/cm^2)**	**Deformation (mm)**
			Air	**Water**	**SSD**									
A		T	B	C	D	E	F	H	I	J	K	L		
Gravity of asphalt binder, G = 0.93						D - C	B / E		(A*F) / G	(H-F) / H *100	I + J	(K-J) / K *100	(2*P) / (π*Q*T)	
5.5	1	61.9	1152.1	675.0	1153.9	478.9	2.406	2.433	14.23	1.1	15.3	92.7	5.4995	0.16
	2	62.1	1150.5	672.4	1151.9	479.5	2.399	2.433	14.19	1.4	15.6	91.1	5.4530	0.25
	3	62.1	1151.6	674.1	1153.3	479.2	2.403	2.433	14.21	1.2	15.4	92.1	5.7505	0.17
	Ave.					479.2	2.403	2.433	14.21	1.2	15.5	92.0	5.6	0.19

Table B5 ITS Test results Hot Mix Asphalt

Hot Mix Asphalt														
Asphalt Content (%)	**No.**	**Height (mm)**	**Weight (g)**			**Volume**	**Bulk Density**	**Theoretical Max. Density**	**Asphalt Volume (%)**	**Air Voids (%)**	**VMA (%)**	**VFA (%)**	**ITS (kg/cm^2)**	**Deformation (mm)**
			Air	**Water**	**SSD**									
A		T	B	C	D	E	F	H	I	J	K	L		
						D - C	B / E		(A*F) / G	(H-F) / H *100	I + J	(K-J) / K *100	(2*P) / (π*Q*T)	
5.5	1	62.7	1153.4	673.2	1155.7	482.5	2.390	2.430	14.14	1.6	15.8	89.7	7.289	0.16
	2	62.7	1151.2	673.5	1153.3	479.8	2.399	2.430	14.19	1.3	15.5	91.8	6.567	0.25
	3	62.0	1152.6	673.9	1154.2	480.3	2.400	2.430	14.19	1.2	15.4	91.9	7.370	0.17
	Ave.					480.9	2.397	2.430	14.17	1.4	15.6	91.1	7.1	0.19

Moisture Sensitivity Test Results

Table B6 Tensile Strength Ratio for Advera WMA

Sample ID	Thickness (cm)	Dry Mass (g)	SSD Mass (g)	Wet Mass (g)	Volume	Bulk. Sp. Gr	Max Sp. Gr.	Air Void (%)	Volume Air Void	MaxLoad (kgf)	ITS (Dry) (kg/cm2)
	T	A	B	C	E	F	G	H	I	P	Std
					(B-C)	(A/E)	G	(100*(G-F)/G)	HE/100		2P/πDT
1	67.0	1147.7	1155.0	648.0	507.0	2.264	2.446	7.5	37.78	553.6	5.2
2	66.8	1151	1158.5	653.2	505.3	2.278	2.446	6.9	34.74	175.2	1.6
3	66.4	1151.6	1158.7	653.8	504.9	2.281	2.446	6.8	34.09	591.9	5.6
4	66.4	1149.8	1157.6	653.3	504.3	2.280	2.446	6.8	34.23	559.1	5.3
5	66.8	1152.0	1158.3	651.9	506.4	2.275	2.446	7.0	35.43	193.8	1.8
6	66.8	1152.1	1159.1	654.2	504.9	2.282	2.446	6.7	33.89	175.6	1.6
Ave.						2.277		6.9	36.26	553.6	5.2

Target Saturation Level: 70 - 80 %

Sample ID	SSD Mass (g)	Wet Mass (g)	Volume	Bulk. Sp. Gr	Vol Abs. Water	% Saturation	MaxLoad (kgf)	ITS (Wet) (kg/cm2)	Tensile Strength Ratio (TSR), %
	B'	C'	E'	F'	J'	S'	P'	Stw	
			(B'-C')	(A/E')	(B'-B)	(100*(J'/I))		2P'/πDT	(Stw/Std) *100
2	1182.9	680.3	502.6	2.290	24.40	70.2	175.2	1.6	**=(5.3/1.7)*100 = 31.85 %**
5	1183.4	681.8	501.6	2.297	25.10	70.8	193.8	1.8	
6	1182.8	680.5	502.3	2.294	23.70	69.9	175.6	1.6	
Ave.				2.294	23.70	69.9		1.7	

Table B7 Tensile Strength Ratio for the Aspha-min (powder)

Sample ID	Thickness (cm)	Dry Mass (g)	SSD Mass (g)	Wet Mass (g)	Volume	Bulk. Sp. Gr	Max Sp. Gr.	Air Void (%)	Volume Air Void	Max_{Load} (kgf)	ITS (Dry) (kg/cm2)
	T	A	B	C	E	F	G	H	I	P	Std
					(B-C)	(A/E)	G	(100*(G-F)/G)	HE/100		2P/πDT
1	66.8	1151.8	1159.8	653.0	506.8	2.273	2.434	6.6	33.59	581.85	5.5
2	66.6	1151.2	1159.6	653.0	506.6	2.272	2.434	6.6	33.63	630.45	5.9
3	66.8	1149.2	1157.8	650.2	507.6	2.264	2.434	7.0	35.46	604.80	5.7
4	66.9	1151.2	1157.7	653.3	504.4	2.282	2.434	6.2	31.43	235.80	2.2
5	66.3	1151.4	1159.5	653.2	506.3	2.274	2.434	6.6	33.25	225.00	2.1
6	66.6	1151.7	1157.5	654.2	503.3	2.288	2.434	6.0	30.13	211.05	2.0
Ave.						2.276		6.5	33.47	414.8	3.9

Target Saturation Level: 70 - 80 %

Sample ID	SSD Mass (g)	Wet Mass (g)	Volume	Bulk. Sp. Gr	Vol Abs. Water	% Saturation	Max_{Load} (kgf)	ITS (Wet) (kg/cm^2)	Tensile Strength Ratio (TSR), %
	B'	C'	E'	F'	J'	S'	P'	Stw	
			(B'-C')	(A/E')	(B'-B)	(100*(J'/I))		2P'/πDT	(Stw/Std) *100
5	1182.8	683	499.8	2.304	23.30	70.1	225.00	2.1	
4	1182.7	683.2	499.5	2.305	25.00	79.5	235.80	2.2	
6	1181.5	682.6	498.9	2.308	24.00	79.7	211.05	2.0	**= (2.1/5.7)*100 = 36.97 %**
Ave.				2.307	24.50	79.6	224.00	2.1	

Table B8 Tensile Strength Ratio for Cecabase RT

Sample ID	Thickness (cm)	Dry Mass (g)	SSD Mass (g)	Wet Mass (g)	Volume	Bulk. Sp. Gr	Max Sp. Gr.	Air Void (%)	Volume Air Void	Max_{Load} (kgf)	ITS (Dry) (kg/cm2)
	T	A	B	C	E	F	G	H	I	P	Std
					(B-C)	(A/E)	G	(100*(G-F)/G)	HE/100		2P/πDT
1	6.67	1149.5	1158.8	654.6	504.2	2.280	2.438	6.5	32.71	265.59	2.5
2	6.69	1151.0	1160.5	651.1	509.4	2.260	2.438	7.3	37.29	266.546	2.5
3	6.68	1150.9	1159.3	652.5	506.8	2.271	2.438	6.9	34.73	574.764	5.4
4	6.68	1148.8	1158.5	651.3	507.2	2.265	2.438	7.1	35.99	529.818	5.0
5	6.69	1152.1	1160.1	652.9	507.2	2.271	2.438	6.8	34.64	268.314	2.5
6	6.682	1150.0	1160.8	652.4	508.4	2.262	2.438	7.2	36.70	543.892	5.1
Ave.						2.268		7.0	35.34	408.2	3.8

Target Saturation Level: 70 - 80 %

Sample ID	SSD Mass (g)	Wet Mass (g)	Volume	Bulk. Sp. Gr	Vol Abs. Water	% Saturation	Max_{Load} (kgf)	ITS (Wet) (kg/cm^2)	Tensile Strength Ratio (TSR), %
	B'	C'	E'	F'	J'	S'	P'	Stw	
			(B'-C')	(A/E')	(B'-B)	(100*(J'/I))		2P'/πDT	(Stw/Std) *100
1	1181.9	686.6	495.3	2.321	23.10	70.6	265.59	2.5	**(5.2/2.5) *100 = 48.51%**
2	1186.9	682.7	504.2	2.283	26.40	70.8	266.546	2.5	
5	1185.0	679.7	505.3	2.280	24.90	71.9	268.314	2.5	
Ave.				2.281	25.65	71.3	266.8	2.5	

Table B9 Tensile Strength Ratio for Aspha-min (granular)

Sample ID	Thickness (cm)	Dry Mass (g)	SSD Mass (g)	Wet Mass (g)	Volume	Bulk. Sp. Gr	Max Sp. Gr.	Air Void (%)	Volume Air Void	Max_{Load} (kgf)	ITS (Dry) (kg/cm2)
	T	A	B	C	E	F	G	H	I	P	Std
					(B-C)	(A/E)	G	(100*(G-F)/G)	HE/100		2P/πDT
1	6.64	1138.7	1147.3	645.3	502.0	2.268	2.433	6.8	33.98	324.68	3.1
2	6.65	1142.1	1151.4	649.2	502.2	2.274	2.433	6.5	32.78	451.24	4.3
3	6.78	1153.5	1162.8	656.0	506.8	2.276	2.433	6.5	32.69	438.98	4.1
4	6.72	1146.9	1156.4	648.4	508.0	2.258	2.433	7.2	36.61	1085.19	10.1
5	6.71	1151.2	1159.7	653.8	505.9	2.276	2.433	6.5	32.74	1037.31	9.7
6	6.7	1143.8	1154.7	650.8	503.9	2.270	2.433	6.7	33.78	1103.90	10.3
Ave.						2.270		6.7	34.01		3.1

Target Saturation Level: 70 - 80 %

Sample ID	SSD Mass (g)	Wet Mass (g)	Volume	Bulk. Sp. Gr	Vol Abs. Water	% Saturation	Max_{Load} (kgf)	ITS (Wet) (kg/cm^2)	Tensile Strength Ratio (TSR), %
	B'	C'	E'	F'	J'	S'	P'	Stw	
			(B'-C')	(A/E')	(B'-B)	(100*(J'/I))		2P'/πDT	(Stw/Std) *100
1	1171.1	674.7	496.4	2.294	23.80	70.0	324.68	3.06	
2	1174.5	675.8	498.7	2.290	23.10	70.5	451.24	4.25	**(3.8/10.04)*100 = 37.75%**
3	1185.7	681.7	504.0	2.289	22.90	70.0	438.98	4.06	
Ave.				2.291	23.267	70.187	404.963	3.791	

Table B10 Tensile Strength Ratio for Hot Mix Asphalt

Sample ID	Thickness (cm)	Dry Mass (g)	SSD Mass (g)	Wet Mass (g)	Volume	Bulk. Sp. Gr	Max Sp. Gr.	Air Void (%)	Volume Air Void	Max_{Load} (kgf)	ITS (Dry) (kg/cm2)
	T	A	B	C	E	F	G	H	I	P	Std
					(B-C)	(A/E)	G	(100*(G-F)/G)	HE/100		2P/πDT
1	66.30	1152.5	1158.5	652.0	506.5	2.275	2.430	6.4	32.22	422.6	3.99
2	66.50	1152.1	1160.9	653.3	507.6	2.270	2.430	6.6	33.48	572.4	5.39
3	66.80	1149.5	1156.6	648.4	508.2	2.262	2.430	6.9	35.15	591.8	5.55
4	65.50	1148.0	1154.2	647.4	506.8	2.265	2.430	6.8	34.37	413.1	3.95
5	66.60	1147.9	1153.3	643.8	509.5	2.253	2.430	7.3	37.11	418.1	3.93
6	66.60	1149.1	1157.9	653.0	504.9	2.276	2.430	6.3	32.02	596.3	5.61
Ave.						2.267	2.430	6.7	33.81		4.69

Target Saturation Level: 70 - 80 %

Sample ID	SSD Mass (g)	Wet Mass (g)	Volume	Bulk. Sp. Gr	Vol Abs. Water	% Saturation	Max_{Load} (kgf)	ITS (Wet) (kg/cm^2)	Tensile Strength Ratio (TSR), %
	B'	C'	E'	F'	J'	S'	P'	Stw	
			(B'-C')	(A/E')	(B'-B)	(100*(J'/I))		2P'/πDT	(Stw/Std) *100
5	1180.2	677.2	503.0	2.282	26.90	72.5	418.1	3.93	**= 4.00/5.52 = 71.76%**
1	1182.7	683.1	499.6	2.307	24.20	75.1	422.6	3.99	
4	1179.6	680.0	499.6	2.298	25.40	73.9	413.1	3.95	
Ave.							417.9	4.0	

Dynamic Modulus Test Results

Table B11 Dynamic Modulus results of Advera WMA at 4.4ºC

Advera WMA at 4.4ºC			
#1	1st Test	2nd Test	Ave.
25	12,114,620	12,626,150	12,370,385
10	10,642,360	10,984,140	10,813,250
5	9,276,605	9,552,860	9,414,733
1	6,167,307	6,346,162	6,256,735
0.5	4,989,066	5,147,049	5,068,058
0.1	3,176,951	3,189,208	3,183,080
#2	1st Test	2nd Test	Ave.
25	15,767,240	15,373,250	15,570,245
10	13,646,320	13,341,100	13,493,710
5	11,961,150	11,571,490	11,766,320
1	8,196,003	7,773,534	7,984,769
0.5	6,702,669	6,270,321	6,486,495
0.1	4,190,528	3,830,891	4,010,710

Table B12 Dynamic Modulus results of Advera WMA at 21.1º C

Advera WMA at 21.1ºC			
#1	1st Test	2nd Test	Ave.
25	5,576,657	5,971,370	5,774,014
10	4,110,971	6,063,031	5,087,001
5	3,203,102	2,953,693	3,078,398
1	1,620,015	1,524,340	1,572,178
0.5	1,232,862	1,199,182	1,216,022
0.1	792,555	791,789	792,172
#2	1st Test	2nd Test	Ave.
25	5,911,202	4,473,726	5,192,464
10	4,232,087	3,155,811	3,693,949
5	3,265,798	2,507,066	2,886,432
1	1,657,512	1,354,448	1,505,980
0.5	1,271,497	1,099,373	1,185,435
0.1	824,411	792,167	808,289

Table B13 Dynamic Modulus results of Advera WMA at 37.8º C

Advera WMA at 37.8ºC			
#1	1st Test	2nd Test	Ave.
25	2,277,724	2,455,430	2,366,577
10	1,454,747	1,987,685	1,721,216
5	1,103,188	1,306,002	1,204,595
1	510,330	552,241	531,285
0.5	355,798	574,550	465,174
0.1	201,412	329,217	265,314
#2	1st Test	2nd Test	Ave.
25	2,333,685	2,941,454	2,637,570
10	1,271,304	1,405,944	1,338,624
5	1,758,407	1,301,923	1,530,165
1	370,019	787,064	578,541
0.5	246,705	532,499	389,602
0.1	283,404	248,911	266,158

Table B14 Dynamic Modulus results of Cecabase RT at 4.4º C

Cecabase RT at 4.4º			
#1	1st Test	2nd Test	Ave.
25	13,110,040	13,215,960	13,163,000
10	11,343,660	11,522,460	11,433,060
5	9,873,085	10,041,200	9,957,143
1	6,567,831	6,824,085	6,695,958
0.5	5,274,294	5,612,427	5,443,361
0.1	3,239,414	3,629,880	3,434,647
#2	1st Test	2nd Test	Ave.
25	11,427,870	12,060,910	11,744,390
10	9,685,835	10,351,260	10,018,548
5	8,320,272	8,935,417	8,627,845
1	5,263,144	5,907,765	5,585,455
0.5	4,177,995	4,787,829	4,482,912
0.1	2,560,932	3,096,077	2,828,505

Table B15 Dynamic Modulus results of Cecabse RT at 21.1º C

Cecabase RT at 21.1º C			
#1	1st Test	2nd Test	Ave.
25	4,666,368	4,456,800	4,561,584
10	3,137,037	3,042,807	3,089,922
5	2,395,656	2,350,078	2,372,867
1	1,233,508	1,161,507	1,197,508
0.5	937,423	921,352	929,387
0.1	609,684	619,052	614,368
#2	1st Test	2nd Test	Ave.
25	5,568,777	5,397,859	5,483,318
10	4,083,909	3,941,594	4,012,752
5	3,237,818	3,124,898	3,181,358
1	1,760,282	1,692,081	1,726,182
0.5	1,405,039	1,355,143	1,380,091
0.1	978,666	933,904	956,285

Table B16 Dynamic Modulus results of Cecabse RT at 37.8º C

Cecabase RT at 37.8º C			
#1	1st Test	2nd Test	Ave.
25	1,379,316	1,459,821	1,419,569
10	1,087,729	1,129,854	1,108,792
5	863,865	829,657	846,761
1	447,395	465,033	456,214
0.5	393,554	397,199	395,377
0.1	300,407	313,101	306,754
#2	1st Test	2nd Test	Ave.
25	1,922,019	2,239,345	2,080,682
10	1,623,736	1,790,289	1,707,013
5	1,308,242	1,449,496	1,378,869
1	724,477	821,796	773,136
0.5	616,772	691,755	654,264
0.1	495,387	540,051	517,719

Table B17 Dynamic Modulus results of Aspha-min (granular) at 4.4º C

Aspha-min (granular) at 4.4ºC			
#1	1st Test	2nd Test	Ave.
25	12,445,230	13,722,720	13,083,975
10	11,392,920	11,912,030	11,652,475
5	9,932,890	10,413,070	10,172,980
1	6,593,164	7,194,248	6,893,706
0.5	5,331,906	5,877,941	5,604,924
0.1	3,324,013	3,718,072	3,521,043
#2	1st Test	2nd Test	Ave.
25	13,264,440	13,142,270	13,203,355
10	11,538,840	11,390,170	11,464,505
5	10,017,900	9,890,879	9,954,390
1	6,617,071	6,580,947	6,599,009
0.5	5,352,780	5,330,636	5,341,708
0.1	3,325,664		3,325,664

Table B18 Dynamic Modulus results of Aspha-min (granular) at 21.1º C

Aspha-min (granular) at 21.1º C			
	1st Test	2nd Test	Ave.
25	5,500,560	5,380,737	5,440,649
10	3,955,627	3,872,991	3,914,309
5	3,107,454	3,026,700	3,067,077
1	1,594,748	1,555,937	1,575,343
0.5	1,245,425	1,223,569	1,234,497
0.1	834,213	813,000	823,606
	1st Test	2nd Test	Ave.
25	4,624,286	4,741,723	4,683,005
10	3,372,208	3,366,415	3,369,312
5	2,647,013	2,612,450	2,629,732
1	1,366,519	1,346,129	1,356,324
0.5	1,083,042	1,076,558	1,079,800
0.1	735,109	725,035	730,072

Table B19 Dynamic Modulus results of Aspha-min (granular) at 37.8º C

Aspha-min at 37.8º C			
#1	1st Test	2nd Test	Ave.
25	1,772,167	1,877,825	1,824,996
10	1,384,257	1,457,234	1,420,746
5	1,002,792	1,067,934	1,035,363
1	546,405	582,953	564,679
0.5	460,436	491,027	475,731
0.1	361,036	382,213	371,624
#2	1st Test	2nd Test	Ave.
25	1,670,189	1,848,212	1,759,201
10	1,294,552	1,420,586	1,357,569
5	948,452	1,044,395	996,424
1	523,308	577,756	550,532
0.5	447,954	488,860	468,407
0.1	354,817	381,553	368,185

Table B20 Dynamic Modulus results of Kumho at 4.4º C

Kumho at 4.4ºC			
#1	1st Test	2nd Test	Ave.
25	12,088,070	11,988,970	12,038,520
10	10,609,110	10,470,510	10,539,810
5	9,310,382	9,160,646	9,235,514
1	6,364,513	6,170,618	6,267,566
0.5	5,210,160	5,026,944	5,118,552
0.1	3,281,575	3,140,687	3,211,131
#2	1st Test	2nd Test	Ave.
25	13,006,750	10,829,630	11,918,190
10	11,448,830	9,006,261	10,227,546
5	9,960,852	7,659,422	8,810,137
1	6,604,521	4,771,288	5,687,905
0.5	5,393,012	3,834,579	4,613,796

Table B21 Dynamic Modulus results of Kumho at 21.1º C

Kumho at 21.1º C			
#1	1st Test	2nd Test	Ave.
25	4,342,133	4,511,927	4,427,030
10	3,461,445	3,106,535	3,283,990
5	2,677,152	2,414,758	2,545,955
1	1,272,650	1,114,445	1,193,548
0.5	990,641	872,714	931,678
0.1	638,390	569,902	604,146
#2	1st Test	2nd Test	Ave.
25	5,030,459	4,933,987	4,982,223
10	3,528,592	3,474,459	3,501,526
5	2,730,817	2,695,834	2,713,326
1	1,305,068	1,303,633	1,304,351
0.5	1,008,111	1,015,463	1,011,787
0.1	649,528	667,609	658,569

Table B22 Dynamic Modulus results of Kumho at 37.8º C

Kumho at 37.8ºC			
#1	1st Test	2nd Test	Ave.
25	1,776,114	2,070,741	1,923,428
10	1,394,415	1,699,065	1,546,740
5	1,043,399	1,111,246	1,077,323
1	518,245	517,451	517,848
0.5	391,791	414,525	403,158
0.1	193,811	166,323	180,067
#2	1st Test	2nd Test	Ave.
25	2,086,548	1,817,356	1,951,952
10	1,847,615	1,211,467	1,529,541
5	1,207,798	1,024,296	1,116,047
1	712,108	587,455	649,781
0.5	390,578	398,455	394,517
0.1	288,003	247,151	267,577

Table B23 Dynamic Modulus results of HMA at 4.4º C

HMA at 4.4º C			
	1st Test	2nd Test	Ave.
25	17,219,940	13,629,440	15,424,690
10	15,267,570	11,959,720	13,613,645
5	13,498,770	10,505,050	12,001,910
1	9,513,511	7,281,031	8,397,271
0.5	7,957,861	5,989,612	6,973,737
0.1	5,137,624	3,842,218	4,489,921
	1st Test	2nd Test	Ave.
25	16,895,540	15,868,870	16,382,205
10	14,878,730	14,307,080	14,592,905
5	13,128,000	12,534,350	12,831,175
1	9,430,113	8,705,658	9,067,886
0.5	7,921,766	7,232,506	7,577,136
0.1	5,173,190	4,697,694	4,935,442

Table B24 Dynamic Modulus results of HMA at 21.1º C

HMA at 21.1º C			
	1st Test	2nd Test	Ave.
25	5,223,361	5,406,155	5,314,758
10	3,708,248	3,944,578	3,826,413
5	2,924,541	3,103,737	3,014,139
1	1,620,623	1,696,485	1,658,554
0.5	1,324,474	1,337,102	1,330,788
0.1	911,443	919,957	915,700
	1st Test	2nd Test	Ave.
25	5,333,377	5,671,729	5,502,553
10	3,907,247	4,141,453	4,024,350
5	3,093,417	3,263,313	3,178,365
1	1,715,129	1,798,862	1,756,996
0.5	1,359,329	1,425,838	1,392,584
0.1	942,708	977,667	960,187

Table B25 Dynamic Modulus results of HMA at 37.8º C

HMA at 37.8º C			
#1	1st Test	2nd Test	Ave.
25	1,748,826	1,936,388	1,842,607
10	1,400,608	1,516,503	1,458,556
5	1,148,784	1,268,732	1,208,758
1	626,853	664,127	645,490
0.5	534,329	559,723	547,026
0.1	435,205	438,882	437,043
#2	1st Test	2nd Test	Ave.
25	1,851,967	1,894,837	1,873,402
10	1,474,903	1,478,604	1,476,754
5	1,222,057	1,220,415	1,221,236
1	665,562	654,685	660,123
0.5	567,168	557,470	562,319
0.1	447,680	446,545	447,112

WORKS CITED

1. AASHTO, *Bulk Specific Gravity of Compacted Bituminous Mixtures Using Saturated Surface-Dry Specimens.* Washington D.C.: American State Highway and Transportation Officials (2001)

2. AASHTO, *Determining Dynamic Modulus of Hot-Mix Asphalt Concrete Mixtures*. Washington D.C.: American Association of State Highway and Transportation Officials (2007)

3. AASHTO *Resistance of Compacted Hot Mix Asphalt (HMA) to Moisture-Induced Damage.* Washington D.C, .American Association of State Highway and Transportation Officials (2007)

4. Abraham T., Christendat D. et al, *Asphaltene-Silica Interactions in Aqueous Solutions: Direct Force Measurements Combined with Electrokinetic Studies*, Industrial and Engineering Chemistry Research, Volume *41*, (2002), pp: 2170-2177.

5. Adedeji A., Grunfelder T. et al, *Asphalt Modified by SBS Triblock Copolymer: Structures and Properties*. Polymer Engineering and Science (1996)

6. Advance Asphalt Technologies, *Mix Design Practices for Warm Mix Asphalt.* National Research Council, Advance Asphalt Technologies. Washington D.C. TRB (2008).

7. Ait-Kadi A., Brahim B.,et al, *Polymer Blends for Enhanced Asphalt binders*, Polymer Engineering and Science, No.12 (1996)

8. Alsteens D., Dague E., *Nanoscale imaging of microbial pathogens using atomic force microscopy,* WIREs Nanomedicine and Nanobiotechnology *, 1*, (2009) pp: 168-180.

9. Bhurke A., Shin E.,et al, *Fracture Morphology and Fracture Toughness Measurement of Polymer-Modified Asphalt Concrete,* Annual meeting of the TRB Draft paper#970942. Washington D.C., TRB (1997)

10. Black, W. R.. *Sustainable transportation: a US Perspective,* Journal of Transport Geography, (1996) pp: 151-159.

11. Binnig G, Quate C.F., Atomic force microscope, Physical Review Letters,(1986) pp: 930–933.

12. Biro S., Gandhi T., et al, *Midrange Temperature Rheological Properties of Warm Asphalt Binder*, Journal of Materials in Civil Engineering *, 21*, (2009) pp: 316-323.

13. Ceca Arkema Group, Retrieved February 15, 2010, from Cecachemicals: http://www.cecachemicals.com/sites/ceca/en/business/bitumen_additives/warm_coated_material/warm_coated_material.page

14. CECA, *CECABASE RT*. Retrieved August 25, 2009, from CECA Arkema Group: http://www.cecachemicals.com/sites/ceca/en/business/bitumen_additives/warm_coated_material/warm_coated_material.page

15. Central Micrscopy, University of Iowa. (2010). *Scanning Probe Microscopy*. Retrieved February 19, 2010, from UI Central Microscopy: http://www.uiowa.edu/~cemrf/methodology/spm/index.htm

16. DOT, Iowa, *Method of Design of Hot Mix Asphalt Mixes.* Ames, Iowa Department of Transportation, (2005)

17. Energy Information Administration, *EIA-Forecast and Analysis*. Retrieved February 25, 2010, from U.S Energy Information Administration Independant Statistics and Analysis (2009): http://www.eia.doe.gov/oiaf/forecasting.html

18. Eurovia Services, *Aspha-min*. Retrieved August 25, 2009, from Eurovia Services: http://www.eurovia.com/en/produit/135.aspx

19. Hurley G., Prowell B., *Evaluation of Aspha-min for use in warm Mix Asphalt.* Auburn, Alabama: National Center for Asphalt Technology (2005)

20. Hurley G., Prowell B., *Evaluation of Sasobit for use in Warm Mix Asphalt.* Auburn, Alabama, National Center for Asphalt Technology (2005)

21. Hurley G., Prowell B., *Evaluation of Evotherm for use in Warm Mix Asphalt.* uburn, Alabama: National Center for Apshalt Technology, (2006)

22. *History of Asphalt*. Retrieved August 26, 2009, from National Asphalt Pavement Association, (2009, March 23): http://www.hotmix.org/index.php?option=com_content&task=view&id=21&Itemid=41

23. *Hot Mix Asphalt Plants Emission Assessment Report.* North Carolina: US Environmental Protection Agency, (2000)

24. Huang J, *Evaluation of Different Techniques for Adhesive Properties of Asphalt-Filler Systems at Interfacial Region,* Journal of ASTM International , Volume 2, (2005)

25. Hurley G., Prowell B., *Evaluation of Potential Process for use in Warm Mix Asphalt.* Journal of the Association of Asphalt Paving Technology (2006)

26. InstroTek, *Maximum Specific Gravity, Gmm, Using the CoreLok method*, Raleigh, NC, USA, (2001, January)

27. Kunnawee K., Sonthong S., et al., *Laboratory Study on Warm Mix Asphalt Additives.* Washington D.C. Presented at 86th Annual Meeting of the Transportation Research Board (2007)

28. Loeber L., Sutton O., et al, *New direct observations of asphalts and asphalt binders by scanning electron microscopy and atomic force microscopy*, Journal of Microscopy,*Volume 182*, (1996), pp: 32-39

29. Lee H., Kim Y., *Use of Warm Mix Asphalt Additives for Cold In - place Recycling using Foamed Asphalt*, Proceedings of the 5th International Conference on Manitenance and Rehabilitation of Pavements and Technological Control, Utah: University of Iowa press (2007)

30. Marti O, Drake B., *Atomic force microscopy of liquid-covered surfaces:atomic resolution images,* Applied Physics Letters, Volume 51, pp: 484–486.

31. Morris V., Kirby A., et al., *Atomic Force Microscopy for Biologists*, Imperial College Press (1999)

32. Masson J., Leblond V., et al., *Bitumin morphologies by phase detection atomic force microscopy*, Journal of Microscopy , 221, (2006), pp: 17-29

33. Newcomb, D. (National Asphalt Pavement Association) Retrieved Decemeber 26, 2009, from fs1.hotmix.org: http://fs1.hotmix.org/mbc/Introduction_to_Warm-mix_Asphalt.pdf

34. Prowell B., Hurley G., *Field Performance of Warm Mix Asphalt at the NCAT Test Track,* Washington D.C., Presented at the 86th annual meeting of the Transportation Research Board (2007)

35. PQ Corporation, *Advera WMA*. Retrieved August 25, 2009, from PQ Corporation: http://www.pqcorp.com/Products/adverawma.asp

36. Roseveld S., Shin E., et al., *Network Morphology of Straight and Polymer Modified Asphalt Cements*, Microscopy Research and Technique, (1997), pp: 529-543.

37. Shin E., Bhurke A., *Microstructure, Morphology, and Failure Modes of Polymer-Modified Asphalt,* Transportation Research Record, No.1535 , (1996), pp: 61-73.

38. Walsh P., *Motor Vehicle Standards and Regulations around the World.* Arlington: Interantional Standards and Regulations, (1999).

39. Wegener L., *Sustainabale Transport*, Journal of Transport Geography, (1997), pp: 177-190.

40. *World Energy council*.. Retrieved October 24, 2009, from World Energy Council (2007, October 5): http://www.worldenergy.org/news__events/media_relations/press_releases/808.asp